
Analyzing Neural Network-Based Generative Diffusion Models through Convex Optimization

Fangzhao Zhang¹ Mert Pilanci¹

Abstract

Diffusion models are becoming widely used in state-of-the-art image, video and audio generation. Score-based diffusion models stand out among these methods, necessitating the estimation of score function of the input data distribution. In this study, we present a theoretical framework to analyze two-layer neural network-based diffusion models by reframing score matching and denoising score matching as convex optimization. Though existing diffusion theory is mainly asymptotic, we characterize the exact predicted score function and establish the convergence result for neural network-based diffusion models with finite data. This work contributes to understanding what neural network-based diffusion model learns in non-asymptotic settings.

1. Introduction

Diffusion models (Sohl-Dickstein et al., 2015) were proposed to tackle the problem of sampling from an unknown distribution and is later shown to be able to generate high quality images (Ho et al., 2020). The work (Song et al., 2021) recognizes the diffusion model as an example of a score-based model which exploit Langevin dynamics to produce data from an unknown distribution. This approach only requires the estimation of the score function of the data distribution. Specifically, the simplest form of Langevin Monte Carlo procedure involves first sampling x^0 from an initial distribution, then repeating the following update

$$x^t \leftarrow x^{t-1} + \frac{\epsilon}{2} \nabla_x \log p(x^{t-1}) + \sqrt{\epsilon} z^t,$$

where z^t is an independently generated i.i.d. Gaussian noise and ϵ is a small constant. Here, $\nabla_x \log p(x)$ is known as the score function of the distribution $p(x)$ we desire to sample from. It can be shown that under certain conditions (Chewi,

2023), we obtain iterates distributed according to the target distribution $p(x)$ as ϵ tends to zero and number of iterations tends to infinity. Langevin dynamics sampling procedure suggests that we can attempt to sample from an unknown distribution as long as we can estimate the score function of this distribution at each data point, which is the key observation in current diffusion models designed for generative tasks. In practice, deep neural networks are trained to minimize variants of score matching objective for fitting the score function.

Existing literature on the theory of diffusion models typically establish convergence of diffusion process when the learned score function approximates the score of unknown data distribution well, but in reality only empirical approximation is available due to finite training samples and limited neural network (NN) capacity. Current literature falls short in understanding the role of NN approximation error for score-based generative models and it is difficult to characterize the distribution from which these models sample in practice. However, in (Pidstrigach, 2022; Yoon et al., 2023; Yi et al., 2023), the authors show NN-based score-based generative models given finite training data does not over-fit due to approximation errors introduced by limited model capacity and also optimization errors.

This work contributes to the understanding neural network approximation error in finite data regime when trained with score matching or denoising score matching objective, which is crucial for understanding neural network-based score-based generative models. Specifically, we answer the following question:

How do NNs approximate the distribution when trained with a (denoising) score matching objective given finite samples and a limited number of neurons?

1.1. Contributions

- We characterize the exact form of predicted score function for two-layer neural networks with finite data samples and establish convergence result for such neural network-based generative models. We are unaware of any prior work solving the same problem. See Section 3.4 for our main convergence results.

¹Department of Electrical Engineering, Stanford University. Correspondence to: Fangzhao Zhang <zfzhang@stanford.edu>.

- We show that the score matching objective can be transformed to a convex program of quadratic form and solved to global optimality for a two-layer neural network. Our convex program for score matching objective bypasses the Jacobian computation issue for piecewise linear activation function such as ReLU, which stabilizes the training procedure and can have practical benefits. See Theorem 3.1 and 3.2 for the derived convex programs.
- We investigate some specific cases where the derived convex program can be solved exactly and carry out simulations to verify our theoretic results. See Section 3.3 for our case study and Section 5.1 for our simulation results.
- We also derive convex programs for two-layer neural networks trained with denoising score matching objective and carry out simulations for verification. See Section 4 for theoretic results and Section 5.2 for simulation results.

1.2. Motivation

We aim to make score matching and denoising score matching via NNs a transparent and reliable tool. Although score matching objective is not as popular as denoising score matching in practice due to scalability issues, the convergence results are cleaner with the score matching objective compared to denoising score matching. In the former case, neural networks are trained to predict scores directly while in latter case neural networks are trained to predict the noise. Moreover, variants such as sliced score matching (Song et al., 2019) are based on the score matching objective and are practical. Thus, understanding neural network approximation error for this objective is still crucial. For denoising score matching, very recent work exists for characterizing shallow neural network prediction (Zeno et al., 2023), however, unlike this paper, the analysis there is not via convexification. Also, our theorem for denoising score matching works for general weight decay while the characterization in (Zeno et al., 2023) works for vanishing weight decay. See Section 2 for a detailed discussion.

1.3. Notation

Here we introduce some notations we will use in later sections. We use $\text{sign}(x)$ to denote the sign function taking value 1 when $x \in [0, \infty)$ and -1 otherwise, and $\mathbb{1}$ to denote the 0-1 valued indicator function taking value 1 when the argument is a true Boolean statement. For any vector x , $\text{sign}(x)$ and $\mathbb{1}\{x \geq 0\}$ applies elementwise. We denote the pseudoinverse of matrix A as A^\dagger . We denote subgradient of a convex function $f : \mathbb{R}^d \rightarrow \mathbb{R}$ at $x \in \mathbb{R}^d$ as $\partial f(x) \subseteq \mathbb{R}^d$.

2. Background

Diffusion model has been shown to be useful in various generative tasks including graph generation (Ho et al., 2020), audio generation (Zhang et al., 2023), and text generation (Wu et al., 2023). Variants of diffusion models such as denoising diffusion implicit model (Song et al., 2022) have been designed to speedup sample generation procedure. The key to score-based diffusion model is the estimation of score function at any data point. In practice, a deep neural network model s_θ is trained to minimize variants of the score matching objective $\mathbb{E}[\|s_\theta(x) - \nabla_x \log p_{\text{data}}(x)\|_2^2]$ and is used for score function estimation. The score matching objective can be shown to be equivalent up to a constant to

$$\mathbb{E}_{p_{\text{data}}(x)} \left[\text{tr}(\nabla_x s_\theta(x)) + \frac{1}{2} \|s_\theta(x)\|_2^2 \right] \quad (1)$$

which is more practical since $\nabla_x \log p_{\text{data}}(x)$ is usually not directly available. To help alleviate the computation overhead in computing trace of Jacobian in (1) for deep neural network and high dimensional data, sliced score matching (Song et al., 2019) which exploits trace estimation method for trace of Jacobian evaluation has been proposed. Another variant is denoising score matching (Vincent, 2011) which considers a perturbed distribution and totally circumvents the computation of trace of Jacobian.

Theory guarantees for diffusion models relate to convergence of log-concave sampling procedure which contains Langevin dynamics. Prior literature establishes convergence of final distribution of log-concave sampling procedure to ground truth data distribution under mild condition with exact score function at each sample point being known (Chewi, 2023). Recent work (Li et al., 2023) characterizes the generalization error for NN-based score models with bounds in number of neurons and obtain vanishing generalization gap when number of neurons tends to infinity, i.e., when the approximation error vanishes. Though neural network approximation error has been recognized to be core to the generalization capability of diffusion models in deep learning, existing work falls short in characterizing the exact score function learned by neural network with finite samples. Our work focuses on analyzing what neural network-based score model learns in finite regime. Specifically, we show that the score matching objective with two-layer neural network score predictor can be reparametrized as a quadratic convex program and solved directly to global optimality and the predicted score function will be piecewise linear with kinks only at training data points. We also investigate simple cases where the convex program can be solved analytically and we observe that the predicted score function may not integrate to be concave and thus only convergence to local stationary point is guaranteed.

Besides theoretic interest mentioned above, our convex pro-

grams may have practical benefit since it stabilizes the training procedure due to convexity. Moreover, for commonly used activation function such as ReLU, trace of Jacobian involves threshold function which has zero gradient almost everywhere. Therefore, conventional gradient-based optimizers may face difficulties minimizing the training objective. Our convex programs bypass this Jacobian computation issue and may thus gain advantage.

To our best knowledge, this is the first work characterizing the exact score function learned by two-layer neural network with finite data samples and this is also the first convex program derived for score-matching objective. Our work is closely related to prior convex neural network theories (Pilanci & Ergen, 2020; Sahiner et al., 2021; Ergen et al., 2023) which consider mainly squared loss instead.

We notice a concurrent work (Zeno et al., 2023) tackling very similar problems as ours though there are several key differences. In (Zeno et al., 2023), the authors study shallow neural network trained for score denoisers and characterize the exact neural network output. The authors show contractive property for NN-based denoiser and prove NN-based denoiser is advantageous against eMMSE denoiser. In our work, we study the exact score matching objective (1) which has not been considered in the other work and establish convergence result for NN-based score predictor which will be much harder to prove for NN-based denoiser due to involvement of noise. Moreover, for denoising score matching objective, we derive convex programs for arbitrary weight decay for multivariate data while the characterization in (Zeno et al., 2023) is for vanishing weight decay. For multivariate data, the authors of (Zeno et al., 2023) only consider modified objective with data belong to special subspaces while our convex programs holds in general. Finally, our analysis is based on convex optimization theory and no convexification is considered in (Zeno et al., 2023). Our work can be viewed as complementary to (Zeno et al., 2023) in the sense that we study similar problems with different objectives and constraints from different angles.

3. Score Matching Objective

In this section, we present the convex programs derived for two-layer neural network. For sake of clarity, we show result for ReLU and absolute value activation with no skip connection. For more general results, see Appendix A.3. We describe the neural network architecture being considered in Section 3.1. Our main theoretic result is presented in Section 3.2, and we investigate some specific cases where the convex program can be solved analytically in Section 3.3.

3.1. Score Matching Problem and Neural Network Architectures

We now describe the training objective and the neural

network architecture being investigated. Let s_θ denote a neural network parameterized by parameter θ with output dimension the same as input data dimension, which is required for score matching estimation. With n data samples, the empirical version of score matching objective (1) is

$$\text{SM}(s_\theta(x)) = \sum_{i=1}^n \text{tr}(\nabla_{x_i} s_\theta(x_i)) + \frac{1}{2} \|s_\theta(x_i)\|_2^2.$$

The final training loss we consider is the above score matching objective together with weight decay term, which writes

$$\min_{\theta} \text{SM}(s_\theta(x)) + \frac{\beta}{2} \|\theta'\|_2^2, \quad (2)$$

where $\theta' \subseteq \theta$ denotes the parameters to be regularized. We note that a non-zero weight decay is indeed core for the optimal value to stay finite, see Appendix A.4 for explanation. Let m denote number of hidden neurons. Consider two-layer neural network of general form as below

$$s_\theta(x) = W^{(2)} \sigma(W^{(1)}x + b^{(1)}) + Vx + b^{(2)}, \quad (3)$$

with activation function σ , parameter $\theta = \{W^{(1)}, b^{(1)}, W^{(2)}, b^{(2)}, V\}$ and $\theta' = \{W^{(1)}, W^{(2)}\}$ where $x \in \mathbb{R}^d$ is the input data, $W^{(1)} \in \mathbb{R}^{m \times d}$ is the first-layer weight, $b^{(1)} \in \mathbb{R}^m$ is the first-layer bias, $W^{(2)} \in \mathbb{R}^{d \times m}$ is the second-layer weight, $b^{(2)} \in \mathbb{R}^d$ is the second-layer bias and $V \in \mathbb{R}^{d \times d}$ is the skip connection coefficient.

3.2. Main Theory

We describe separately the derived convex program for univariate data and multivariate in two subsections here, though the former one is included in the later one as a special case. Our case study in Section 3.3 is for univariate data and thus presenting the univariate data convex program explicitly helps improve readability.

3.2.1. UNIVARIATE DATA

We consider training data $x_1, \dots, x_n \in \mathbb{R}$. The following theorem gives the convex program equivalent to the score matching objective (2) for univariate data.

Theorem 3.1. *When σ is ReLU or absolute value activation and $V = 0$, denote the optimal score matching objective value (2) with s_θ specified in (3) as p^* , when $m \geq m^*$ and $\beta \geq 1^1$,*

$$p^* = \min_y \frac{1}{2} \|Ay\|_2^2 + b^T y + \beta \|y\|_1, \quad (4)$$

¹Note when $\beta < 1$, the optimal value to problem (2) is unbounded, see Appendix A.4 for explanation.

where $m^* = \|y^*\|_0$, and y^* is any optimal solution to (4). A, b and reconstruction rule for optimal θ is given in Appendix A.2.

Proof. See Appendix A.2. \square

Here we present the reconstruction rule for absolute value activation for demonstration, see Appendix A.2 and A.3 for other model types. Once an optimal solution y^* to problem (4) has been derived, for any input \tilde{x} , the optimal neural network prediction is given by

$$\tilde{y}(\tilde{x}) = \sum_{i=1}^n (|y_i^*| + |y_{i+n}^*|) |\tilde{x} - x_i| + b_0^*,$$

see Appendix A.3.1 for value of b_0^* . Note the optimal score is a piecewise linear function with breakpoints only at a subset of data points. When training data points are highly separated, the optimal score approximately corresponds to score of mixture of Gaussian with centroids at $\{\tilde{x} : \tilde{y}(\tilde{x}) = 0\}$. Moreover, the breakpoints correspond to the extreme points in each Gaussian component. See Figure 6 in Appendix A.3.1 for score functions for single Gaussian distribution and Gaussian mixture distribution with separated centroids.

3.2.2. MULTIVARIATE DATA

To state the convex program for multivariate data, we first introduce the concept of arrangement matrices. When d is arbitrary, for data matrix $X \in \mathbb{R}^{n \times d}$ and any arbitrary vector $u \in \mathbb{R}^d$, We consider the set of diagonal matrices

$$\mathcal{D} := \{\text{diag}(\mathbb{1}\{Xu \geq 0\})\},$$

which takes value 1 or 0 along the diagonal that indicates the set of possible arrangement activation patterns for the ReLU activation. Indeed, we can enumerate the set of sign patterns as $\mathcal{D} = \{D_i\}_{i=1}^P$ where P is bounded by

$$P \leq 2r \binom{e(n-1)}{r}$$

for $r = \text{rank}(X)$ (Pilanci & Ergen, 2020; Stanley et al., 2004). Now we are ready to present the convex program for multivariate data below. Since the proof of Theorem 3.1 is closely tied to reconstruction of optimal neurons and does not trivially extend to multivariate data, we instead follow (Mishkin et al., 2022) and employ an alternative duality-free proof for Theorem 3.2 to derive

Theorem 3.2. *When σ is ReLU, $V = 0$ and $\beta = 0$, denote the optimal score matching objective value (2) with s_θ specified in (3) as p^* , when $m \geq 2Pd$, under Assumption A.8,*

$$p^* = \min_{W_i} \frac{1}{2} \left\| \sum_{i=1}^P D_i X W_i \right\|_F^2 + \sum_{i=1}^P \text{tr}(D_i) \text{tr}(W_i), \quad (5)$$

where $W_i \in \mathbb{R}^{d \times d}$.

Proof. See Appendix A.9.1. \square

See Appendix A.9 for convex program for more model types. Denote $\tilde{V} = [\text{tr}(D_1)I, \text{tr}(D_2)I, \dots, \text{tr}(D_P)I]$, $W = [W_1, \dots, W_P]^T$, $\tilde{X} = [D_1X, \dots, D_PX]$, then the convex program (5) can be rewritten as

$$\min_W \frac{1}{2} \|\tilde{X}W\|_F^2 + \langle \tilde{V}, W \rangle. \quad (6)$$

When the optimal value is finite, e.g., $\tilde{V} \in \text{range}(\tilde{X}^T \tilde{X})$, an optimal solution to (6) is given by

$$W = (\tilde{X}^T \tilde{X})^\dagger \tilde{V} = \begin{bmatrix} \sum_{k \in S_{11}} X_k X_k^T & \sum_{k \in S_{12}} X_k X_k^T & \cdots \\ \sum_{k \in S_{21}} X_k X_k^T & \sum_{k \in S_{22}} X_k X_k^T & \cdots \\ \cdots & \cdots & \cdots \end{bmatrix}^\dagger \begin{bmatrix} \text{tr}(D_1)I \\ \text{tr}(D_2)I \\ \vdots \\ \text{tr}(D_P)I \end{bmatrix},$$

where $S_{ij} = \{k : X_k^T u_i \geq 0, X_k^T u_j \geq 0\}$ and u_i is the generator of $D_i = \text{diag}(\mathbb{1}\{X u_i \geq 0\})$.

Remark 3.3. Note that the above model can be seen as a piecewise empirical covariance estimator which partitions the space with hyperplane arrangements. When $P = 1$, $D_1 = I$ and $X^T X$ is invertible, then $(\tilde{X}^T \tilde{X})^\dagger$ reduces to the empirical precision matrix which models the correlation between different data points. This was observed in the application of score matching objective in graphical models (Hyvärinen, 2005; Lin et al., 2016) with NNs with linear activation. Here, we obtain a more expressive model with non-linear neural network through data partitioning.

3.3. Special Case: Large Weight Decay Regime

In this section, we investigate convex program (4) assuming training data $x_1, \dots, x_n \in \mathbb{R}$ are distinct. We show that for large β , program (4) can be solved analytically and the integration of predicted score function is always concave for ReLU activation, which aligns with theoretic assumptions for log-concave sampling procedures. Note this does not happen for absolute value activation, where the predicted score function may integrate to be non-concave and only convergence to stationary points holds in this regime.

Consider convex program (4). For NNs with ReLU activation and without skip connection, $A \in \mathbb{R}^{n \times 4n}$ and $y \in \mathbb{R}^{4n}$. When $\beta > \|b\|_\infty$, $y = 0$ is optimal and the neural network will always output zero. When $\beta_1 < \beta \leq \|b\|_\infty$ for some threshold β_1^2 , y is all zero except for the first and the $3n$ -th entry, which have value $(\beta - n)/2nv + t$ and $(n - \beta)/2nv + t$ for any $|t| \leq \frac{n - \beta}{2nv}$ correspondingly, see Appendix A.5 for

²See Appendix A.5 for value of β_1 .

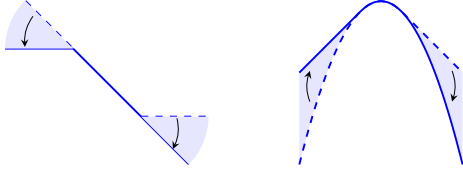


Figure 1. Predicted score function (left) and its integration (right) for univariate data for two-layer ReLU neural network. The left plot shows all optimal score predictions by convex score predictor for weight decay parameter $\beta_1 < \beta \leq n$ and for univariate input data of arbitrary distribution. See Section 3.3 for details.

proof. For any input data point \hat{x} , the predicted score \hat{y} is

$$\begin{cases} \hat{y} = \frac{\beta-n}{nv}(\hat{x} - \mu), & x_1 \leq \hat{x} \leq x_n \\ \hat{y} = -\left(\frac{n-\beta}{2nv} + t\right)\hat{x} + \left(\frac{\beta-n}{2nv} + t\right)x_1 + \frac{n-\beta}{nv}\mu, & \hat{x} < x_1 \\ \hat{y} = \left(\frac{\beta-n}{2nv} + t\right)\hat{x} - \left(\frac{n-\beta}{2nv} + t\right)x_n + \frac{n-\beta}{nv}\mu, & \hat{x} > x_n \end{cases} \quad (7)$$

for some $|t| \leq \frac{n-\beta}{2nv}$, where $\mu = \sum_{i=1}^n x_i/n$ denotes the sample mean and $v = \sum_{i=1}^n (x_i - \mu)^2/n$ denotes the sample variance.

Figure 1 shows the score function prediction of (7) and its integration. Note within sampled data range, the predicted score function aligns with score function of Gaussian distribution parameterized by sample mean μ and sample variance v ; outside data range, the predicted score function is a linear interpolation. The integration of score function is always concave in this case, and therefore Langevin dynamics sampling with predicted score function has well-established convergence guarantees (Durmus & Moulines, 2016a; Dalalyan, 2016; Durmus & Moulines, 2016b). Here we make a comparison with the predicted score for neural network with absolute value activation without skip connection, when β goes below n (see Appendix A.6.1 for details), for any test data \hat{x} , the corresponding predicted score \hat{y} is given by

$$\begin{cases} \hat{y} = \frac{\beta-n}{nv}(\hat{x} - \mu), & x_1 \leq \hat{x} \leq x_n, \\ \hat{y} = -2t\hat{x} + \left(\frac{\beta-n}{nv} + 2t\right)x_1 + \frac{n-\beta}{nv}\mu, & \hat{x} < x_1, \\ \hat{y} = 2t\hat{x} - \left(\frac{n-\beta}{nv} + 2t\right)x_n + \frac{n-\beta}{nv}\mu, & \hat{x} > x_n. \end{cases}$$

Figure 2 depicts the score prediction and its integration. Within the sampled data range, the score prediction corresponds to score of Gaussian distribution parameterized by sample mean and sample variance which is the same as the score predicted by ReLU neural network. The score prediction outside sampled data range is a linear interpolation with a different slope from what is predicted by the ReLU neural network. This underscores the distinction between absolute value activation and ReLU activation. The corresponding probability density is log-concave only when $t = 0$. Notably, the solution with $t = 0$ corresponds to

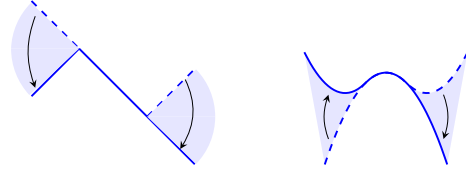


Figure 2. Predicted score function (left) and its integration (right) for univariate data for two-layer absolute value activation neural network. The left plot shows all optimal score predictions by convex score predictor for weight decay parameter $\beta_2 < \beta \leq n$ and for univariate input data of arbitrary distribution. See Section 3.3 for details.

the unique minimum norm solution of the convex program (4), highlighting its significance. Here the score prediction no longer corresponds to log-concave distribution except for the min-norm case and classic convergence theory has only theoretic assurance for converging to stationary points (Chewi, 2023). When it comes to difference between neural networks with and without skip connection, for large $\beta > n$, the optimal score prediction is all zeros for NNs without skip connection. When skip connection is added, the optimal score prediction is no longer zero and the corresponding neural network parameter set is given by $\{W^{(1)} = 0, b^{(1)} = 0, W^{(2)} = 0, b^{(2)} = \mu/v, V = -1/v\}$. For any test data \hat{x} , the corresponding predicted score is given by

$$\hat{y} = V\hat{x} + b^{(2)} = -\frac{1}{v}(\hat{x} - \mu),$$

which gives the score function of Gaussian distribution with mean being sample mean and variance being sample variance. Therefore, adding skip connection would change the zero score prediction to a linear function parameterized by sample mean and variance in the large weight decay regime. See Appendix A.6.2 and A.6.3 for details.

3.4. Convergence Result

Consider two-layer ReLU network without skip connection and training points $x_1, \dots, x_n \in \mathbb{R}$. For neural network-based score function predictor, note once $y^* \in \mathbb{R}^{4n}$ to the convex program (4) is known, for any input data x , the score prediction is given by

$$s(x) = \sum_{i=1}^n y_i'^{*T} \mathcal{D}(x, x_i) + b_0^*,$$

where $y_i'^* \in \mathbb{R}^4$ is constant expressed in y^* , $\mathcal{D}(x, x_i) \in \mathbb{R}^4$ is entrywise piecewise linear with kinks at x_i . b_0^* is constant. See Appendix A.8 for definition of $y_i'^*$, $\mathcal{D}(\cdot)$ and b_0^* . Integrating the above score function we get

$$\int s(x)dx = \frac{1}{2} \sum_{i=1}^n y_i'^{*T} \mathcal{D}^2(x, x_i) + b_0^*x.$$

The corresponding probability density is proportional to

$$\exp\left(\int s(x)dx\right) = \exp\left(\frac{1}{2}\sum_{i=1}^n y_i^{*T} \mathcal{D}^2(x, x_i) + b_0^*x\right).$$

Note that the log-density is piecewise quadratic with break-points only at a subset of training points.

Strong convergence guarantees for Langevin Monte Carlo method are often contingent upon the log-concavity of the target distribution. Notably, in Section 3.3 we analyze the predicted score function in certain ranges of weight decay. These score functions correspond to log concave distributions for ReLU activation and thus we can exploit existing convergence results for Langevin dynamics to derive the convergence of diffusion model with a neural network-based score function. Here, we follow notations used in Section 3.3. Algorithms of score matching and Langevin sampling are given in Algorithm 1 and 2 respectively. To the best of our knowledge, prior to our study, there has been no characterization of the sample distribution generated by Algorithm 2 when the score model is trained using Algorithm 1.

Algorithm 1 Score Matching

Input: training data $x_1, \dots, x_n \in \mathbb{R}^d$
minimize

$$\sum_{i=1}^n \frac{1}{2} s_\theta^2(x_i) + \nabla_\theta s_\theta(x_i) + \frac{\beta}{2} \|\theta'\|_2^2$$

Theorem 3.4. *When s_θ is of two-layer ReLU and $\beta_1^3 < \beta \leq n$, let π denote the target distribution (defined below). For any $\epsilon \in [0, 1]$, if we take step size $\eta \asymp \frac{\epsilon^2 nv}{n-\beta}$, then for the mixture distribution $\bar{\mu} = T^{-1} \sum_{t=1}^T x^t$, it holds that $\sqrt{\text{KL}(\bar{\mu} \parallel \pi)} \leq \epsilon$ after*

$$O\left(\frac{(n-\beta)W_2^2(\mu_0, \pi)}{nv\epsilon^4}\right) \text{ iterations,}$$

where W_2 denotes 2-Wasserstein distance and π satisfies

$$\pi \propto \begin{cases} \exp\left(\left(\frac{\beta-n}{4nv} - \frac{t}{2}\right)x^2 + \left(\frac{\beta-n}{2nv} + t\right)x_1x\right. \\ \quad \left. + \left(\frac{\mu(n-\beta)}{nv}\right)x + \left(\frac{n-\beta}{4nv} - \frac{t}{2}\right)x_1^2\right), & x < x_1, \\ \exp\left(\frac{\beta-n}{2nv}x^2 - \frac{\mu(\beta-n)}{nv}x\right), & x_1 \leq x \leq x_n, \\ \exp\left(\left(\frac{\beta-n}{4nv} + \frac{t}{2}\right)x^2 - \left(\frac{n-\beta}{2nv} + t\right)x_nx\right. \\ \quad \left. + \left(\frac{\mu(n-\beta)}{nv}\right)x + \left(\frac{t}{2} + \frac{n-\beta}{4nv}\right)x_n^2\right), & x \geq x_n, \end{cases}$$

for some $|t| \leq \frac{n-\beta}{2nv}$.

Proof. See Appendix A.8. \square

³See Section 3.3 for value of β_1

Theorem 3.4 is a simple extension of prior literature for log-concave sampling convergence given we derive the NN-predicted score and the distribution it characterizes is indeed log-concave.

Algorithm 2 Langevin Monte Carlo

Initialize: $x^0 \sim \mu_0(x)$
for $t = 1, 2, \dots, T$ **do**
 $z^t \sim \mathcal{N}(0, 1)$
 $x^t \leftarrow x^{t-1} + \frac{\epsilon}{2} s_\theta(x^{t-1}) + \sqrt{\epsilon} z^t$
end for

4. Denoising Score Matching Objective

To tackle the difficulty in computation of trace of Jacobian required in score matching objective (1), denoising score matching has been proposed in (Vincent, 2011). It then becomes widely used in practical generative models. In this section, we derive convex programs for the denoising score matching objective.

To briefly introduce, denoising score matching first perturbs data points with a predefined noise distribution and then estimates the score of the perturbed data distribution. When the noise distribution is chosen to be standard Gaussian, for some noise level $\epsilon > 0$, the objective is equivalent to

$$\min_{\theta} \mathbb{E}_{x \sim p(x)} \mathbb{E}_{\delta \sim \mathcal{N}(0, I)} \left\| s_\theta(x + \epsilon\delta) - \frac{\delta}{\epsilon} \right\|_2^2,$$

and the empirical version is given by

$$\text{DSM}(s_\theta) = \sum_{i=1}^n \frac{1}{2} \left\| s_\theta(x_i + \epsilon\delta_i) - \frac{\delta_i}{\epsilon} \right\|_2^2, \quad (8)$$

where $\{x_i\}_{i=1}^n$ are samples from $p(x)$ and $\{\delta_i\}_{i=1}^n$ are samples from standard Gaussian. The final training loss we consider is the above score matching objective together with weight decay term, which writes

$$\min_{\theta} \text{DSM}(s_\theta(x)) + \frac{\beta}{2} \|\theta'\|_2^2, \quad (9)$$

where $\theta' \subseteq \theta$ denotes the parameters to be regularized. Unlike for score matching objective where weight decay is important for optimal objective value to stay finite, here for denoising objective, weight decay is unnecessary and can be removed. In our derived convex program, we allow β to be arbitrarily close to zero so the result is general. Note (9) circumvents the computation of trace of Jacobian and is thus more applicable for training tasks in large data regime. One drawback is that optimal s_θ that minimizes (9) measures score function of the perturbed data and is only close to original data distribution when noise is small enough. We consider the same neural network architecture described in Section 3.1.

4.1. Univariate Data

We follow similar analysis pattern as in Section 3 and consider univariate data first. The following theorem states the convex program for denoising score matching objective (9) for univariate data with two-layer ReLU neural network. See Appendix B.2 for convex programs for more model architectures.

Theorem 4.1. *When σ is ReLU and $V = 0$, denote the optimal denoising score matching objective value (9) with s_θ specified in (3) as p^* , when $\beta > 0$ and $m \geq m^*$,*

$$p^* = \min_y \frac{1}{2} \|Ay + b\|_2^2 + \beta \|y\|_1, \quad (10)$$

where $m^* = \|y^*\|_0$, and y^* is any optimal solution to (10). A, b is specified in Appendix B.1.

Proof. See Appendix B.1. \square

Once an optimal y^* of convex program (10) has been obtained, the optimal score prediction for any input x is given by

$$s_{\theta^*}(x) = - \sum_{i=1}^n y_i^* (x - x_i)_+ - \sum_{i=1}^n y_{n+i}^* (-x + x_i)_+ + b_0^*,$$

with $b_0^* = \frac{1}{n} 1^T ([A_1, A_2] y^* + l)$ where $[A_1]_{ij} = (x_i - x_j)_+$ and $[A_2]_{ij} = (-x_i + x_j)_+$. l is the label vector, i.e. $l = [\delta_1/\epsilon, \delta_2/\epsilon, \dots, \delta_n/\epsilon]^T$.

4.2. Multivariate Data

Now we consider multivariate data regime. The below theorem gives the convex program equivalent to the denoising score matching objective (9) for multivariate data. Let $L \in \mathbb{R}^{n \times d}$ denote the label matrix, i.e., $L_i = \delta_i/\epsilon$, and $\mathcal{D} = \{D_i\}_{i=1}^P$ be the arrangement activation patterns for ReLU activation as defined in Section 3.2.2. See Appendix B.3 for convex programs for more model types.

Theorem 4.2. *When σ is ReLU, $V = 0$ and $\beta = 0$, denote the optimal denoising score matching objective value (9) with s_θ specified in (3) as p^* , when $m \geq 2Pd$, under Assumption A.8,*

$$p^* = \min_{W_i} \frac{1}{2} \left\| \sum_{i=1}^P D_i X W_i - L \right\|_F^2, \quad (11)$$

where $W_i \in \mathbb{R}^{d \times d}$.

Proof. see Appendix B.3. \square

Note the derived convex program (11) is a simple quadratic program and any convex program solver can be used to solve it efficiently.

5. Numerical Results

We present score matching objective simulation results in Section 5.1 and denoising score matching objective simulation in Section 5.2, see Appendix C for additional simulations for different model types and for uniformly distributed training data.

5.1. Score Matching Objective

For univariate data and two-layer neural network with ReLU activation considered in Section 3.2.1, Figure 3 shows our simulation results for score matching tasks. We take $n = 500$ data points sampled from standard Gaussian and we take weight decay parameter $\beta = \|b\|_\infty - 1$.⁴ The left plot in Figure 3 shows the training loss where the dashed blue line is the objective value obtained by convex score predictor (4). We solve the convex program analytically as analyzed in Section 3.3 and plot the optimal value. For non-convex neural network training, we run 10 trials with random parameter initiation and use Adam as optimizer with step size $1e-2$. We train for 500 epochs. The result shows that our convex program solves the training problem globally and stably. The middle plot in Figure 3 is the score prediction given by convex neural network, which confirms our derived score function (7). The right plot shows the histogram for running Langevin dynamics sampling in Algorithm 2 with convex score predictor with 10^5 data points and $T = 500$ iterations, we take μ_0 to be uniform distribution from -10 to 10 and $\epsilon = 1$. Note our convex score predictor recover the ground truth data distribution here.

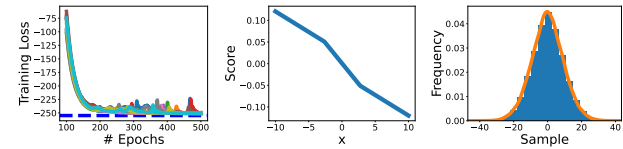


Figure 3. Simulation results for score matching tasks with two-layer ReLU neural network (Gaussian data). The left plot shows training loss where the dashed blue line indicates loss of convex score predictor (4). The middle plot shows score prediction by convex score predictor, which confirms our analysis in Section 3.3. The right plot shows sampling histogram via Langevin process with convex score predictor.

We also test our convex predictor with Gaussian mixture distribution with two separate centroids. The result is shown in Figure 4. Here we take $\beta = 20$ since we know large β would not generate Gaussian mixture score according to our analysis in Section 3.3. Note our convex score predictor produces the optimal training loss and recovers the ground truth Gaussian mixture distribution.

⁴See Section 3.2.1 for definition of b .

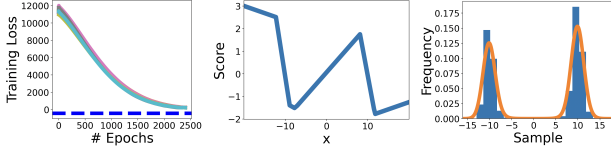


Figure 4. Simulation results for score matching tasks with two-layer ReLU neural network (Gaussian mixture data). The left plot shows training loss where the dashed blue line indicates loss of convex score predictor (4). The middle plot shows score prediction by convex score predictor. The right plot shows sampling histogram via Langevin process with convex score predictor. The ground truth distribution is Gaussian mixture with two centroids centered at -10 and 10 respectively and with unit variance, which is recovered by our model.

5.2. Denoising Score Matching Objective

Figure 5 shows our simulation results for denoising score matching tasks. The upper left plot shows denoising score matching training loss where the dashed blue line indicates the loss of convex score predictor from our derived convex program (10) solved with CVXPY. We take weight decay parameter $\beta = 0.5$, $n = 1000$ data points with standard Gaussian distribution, and noise level $\epsilon = 0.1$ in (8). The non-convex training uses Adam with step size $1e - 2$ and takes 200 epochs. We run 10 trials. The notable gap between non-convex training loss and the convex score predictor loss reveals that our convex program solves the training problem globally and stably. The rest plots show the histogram for samples generated via annealed Langevin process (Algorithm 3) with non-convex score predictor and convex score predictor respectively. See Appendix C.2 for experimental hyperparameter choices.

Algorithm 3 Annealed Langevin Sampling

Initialize: $\epsilon_0, \sigma_1, \dots, \sigma_L, x^0 \sim \mu_0(x)$
for $i = 1, 2, \dots, L$ **do**
 $\epsilon_i = \epsilon_0 \sigma_i^2 / \sigma_L^2$
for $t = 1, 2, \dots, T$ **do**
 $z^t \sim \mathcal{N}(0, 1)$
 $x^t \leftarrow x^{t-1} + \frac{\epsilon_i}{2} s_{\theta_i}(x^{t-1}) + \sqrt{\epsilon_i} z^t$
end for
end for

The first histogram shows the generation result with convex score predictor, the third, fourth, and fifth histograms show sampling results with non-convex score predictor corresponding to learning rates $1, 1e - 2, 1e - 6$ respectively. The first histogram resembles the ground truth Gaussian distribution well while the sampling quality with non-convex score predictor depends heavily on the learning rate choice, which reveal that our convex program is helpful for producing high quality samples stably.

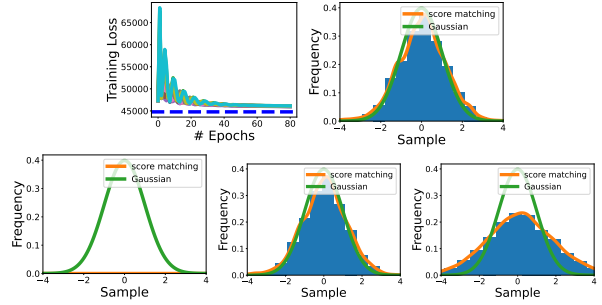


Figure 5. Simulation results for denoising score matching tasks with two-layer ReLU neural network. The upper left plot shows training loss where the dashed blue line indicates loss of convex score predictor (10). The second plot shows sampling histogram via annealed Langevin process with convex score predictor. The third, fourth, and fifth plots show sampling histograms via annealed Langevin process with non-convex score predictors trained with learning rates $1, 1e - 2, 1e - 6$ respectively. The ground truth distribution is standard Gaussian, which is recovered by our model.

6. Conclusion

In this work, we analyze neural network-based diffusion models via lens of convex optimization. We derive an equivalent convex program for two-layer neural networks trained using the score matching objective, which solves the problem globally and bypasses the difficulty of using gradient-based optimizers due to the Jacobian terms. We also derive the convex program for denoising score matching objective. When data is univariate, we find the optimal set of the convex program for the score matching objective for certain weight decay range, and show that for arbitrary data distributions, the neural network-learned score function is piecewise linear and can always be parameterized by sample mean and sample variance. We established convergence results for Langevin sampling with neural network-learned score function.

7. Limitations

In this work, we derive the convex program for score matching objective and denoising score matching objective with weight decay. Though our results hold for general weight decay that can be taken arbitrarily small except for score matching objective where we require reasonable weight decay bound (see Section 3.2.1 for discussion), our convex program always picks the neural network with minimal representation cost. The inductive bias of min-cost NN is not covered in this work. We note that recent work shows stable SGD minimizer has low representation cost (Mulayoff et al., 2021; Nacson et al., 2023). Initializing the weights randomly with small magnitude and running a local optimizer has also been shown to have the same effect as penalizing the weight decay term (Wang & Pilanci, 2021).

Our theory studies shallow two-layer neural network and we leave the extension to deeper NNs as future work. Recent development of convex neural network theory for deeper NNs may provide some insights (Ergen & Pilanci, 2021).

8. Acknowledgements

This work was supported in part by the National Science Foundation (NSF) under Grant DMS-2134248; in part by the NSF CAREER Award under Grant CCF-2236829; in part by the U.S. Army Research Office Early Career Award under Grant W911NF-21-1-0242; in part by the Precourt Institute for Energy and the SystemX Alliance at Stanford University.

References

- Chewi, S. Log-concave sampling, 2023. URL <https://chewisinho.github.io/main.pdf>.
- Dalalyan, A. S. Theoretical guarantees for approximate sampling from smooth and log-concave densities, 2016.
- Durmus, A. and Moulines, É. Sampling from a strongly log-concave distribution with the unadjusted langevin algorithm. *arXiv: Statistics Theory*, 2016a. URL <https://api.semanticscholar.org/CorpusID:124591590>.
- Durmus, A. and Moulines, E. Non-asymptotic convergence analysis for the unadjusted langevin algorithm, 2016b.
- Ergen, T. and Pilanci, M. Revealing the structure of deep neural networks via convex duality. In Meila, M. and Zhang, T. (eds.), *Proceedings of the 38th International Conference on Machine Learning*, volume 139 of *Proceedings of Machine Learning Research*, pp. 3004–3014. PMLR, 18–24 Jul 2021.
- Ergen, T., Gulluk, H. I., Lacotte, J., and Pilanci, M. Globally optimal training of neural networks with threshold activation functions, 2023.
- Ho, J., Jain, A., and Abbeel, P. Denoising diffusion probabilistic models, 2020.
- Hyvärinen, A. Estimation of non-normalized statistical models by score matching. *Journal of Machine Learning Research*, 6(24):695–709, 2005. URL <http://jmlr.org/papers/v6/hyvarinen05a.html>.
- Li, P., Li, Z., Zhang, H., and Bian, J. On the generalization properties of diffusion models, 2023.
- Lin, L., Drton, M., and Shojaie, A. Estimation of high-dimensional graphical models using regularized score matching, 2016.
- Mishkin, A., Sahiner, A., and Pilanci, M. Fast convex optimization for two-layer relu networks: Equivalent model classes and cone decompositions, 2022.
- Mulayoff, R., Michaeli, T., and Soudry, D. The implicit bias of minima stability: A view from function space. In Beygelzimer, A., Dauphin, Y., Liang, P., and Vaughan, J. W. (eds.), *Advances in Neural Information Processing Systems*, 2021. URL <https://openreview.net/forum?id=2STmSnZAet2>.
- Nacson, M. S., Mulayoff, R., Ongie, G., Michaeli, T., and Soudry, D. The implicit bias of minima stability in multivariate shallow relu networks, 2023.
- Pidstrigach, J. Score-based generative models detect manifolds, 2022.
- Pilanci, M. and Ergen, T. Neural networks are convex regularizers: Exact polynomial-time convex optimization formulations for two-layer networks, 2020.
- Sahiner, A., Ergen, T., Pauly, J., and Pilanci, M. Vector-output relu neural network problems are copositive programs: Convex analysis of two layer networks and polynomial-time algorithms, 2021.
- Sohl-Dickstein, J., Weiss, E. A., Maheswaranathan, N., and Ganguli, S. Deep unsupervised learning using nonequilibrium thermodynamics, 2015.
- Song, J., Meng, C., and Ermon, S. Denoising diffusion implicit models, 2022.
- Song, Y., Garg, S., Shi, J., and Ermon, S. Sliced score matching: A scalable approach to density and score estimation, 2019.
- Song, Y., Sohl-Dickstein, J., Kingma, D. P., Kumar, A., Ermon, S., and Poole, B. Score-based generative modeling through stochastic differential equations, 2021.
- Stanley, R. P. et al. An introduction to hyperplane arrangements. *Geometric combinatorics*, 13(389-496):24, 2004.
- Vincent, P. A connection between score matching and denoising autoencoders. *Neural computation*, 23(7):1661–1674, 2011.
- Wang, Y. and Pilanci, M. The convex geometry of back-propagation: Neural network gradient flows converge to extreme points of the dual convex program, 2021.
- Wu, T., Fan, Z., Liu, X., Gong, Y., Shen, Y., Jiao, J., Zheng, H.-T., Li, J., Wei, Z., Guo, J., Duan, N., and Chen, W. Ar-diffusion: Auto-regressive diffusion model for text generation, 2023.

Yi, M., Sun, J., and Li, Z. On the generalization of diffusion model, 2023.

Yoon, T., Choi, J. Y., Kwon, S., and Ryu, E. K. Diffusion probabilistic models generalize when they fail to memorize. In *ICML 2023 Workshop on Structured Probabilistic Inference & Generative Modeling*, 2023. URL <https://openreview.net/forum?id=shciCbSk9h>.

Zeno, C., Ongie, G., Blumenfeld, Y., Weinberger, N., and Soudry, D. How do minimum-norm shallow denoisers look in function space?, 2023.

Zhang, C., Zhang, C., Zheng, S., Zhang, M., Qamar, M., Bae, S.-H., and Kweon, I. S. A survey on audio diffusion models: Text to speech synthesis and enhancement in generative ai, 2023.

A. Supplementary Theoretic Materials for Section 3

A.1. Technical Lemmas

Lemma A.1. *The below constraint set is strictly feasible only when $\beta > 1$.*

$$\begin{cases} |z^T(x - 1x_i)_+ - 1^T \mathbb{1}\{x - 1x_i \geq 0\}| \leq \beta \\ |z^T(x - 1x_i)_+ - 1^T \mathbb{1}\{x - 1x_i > 0\}| \leq \beta \\ |z^T(-x + 1x_i)_+ + 1^T \mathbb{1}\{-x + 1x_i \geq 0\}| \leq \beta \\ |z^T(-x + 1x_i)_+ + 1^T \mathbb{1}\{-x + 1x_i > 0\}| \leq \beta \\ z^T \mathbf{1} = 0 \end{cases} \quad \forall i = 1, \dots, n$$

Proof. Consider without loss of generality that $x_1 < x_2 < \dots < x_n$. Let $k = -\sum_{j=1}^m z_j(x_j - x_i) + m$ for some $1 \leq m \leq n$, the first four constraints with $i = m$ are then $|z^T x - (n+1) + k|, |z^T x - (n+1) + k + 1|, |k|, |k - 1|$. When $i = n$, the first constraint is $\beta \geq 1$. Thus $\beta > 1$ is necessary for the constraint set to be strictly feasible. Since we can always find z^* satisfying

$$\begin{cases} x^T z^* = n \\ 1^T z^* = 0 \\ (x - 1x_i)_+^T z^* - 1^T \mathbb{1}\{x - 1x_i \geq 0\} = 0 \quad \forall i = 2, \dots, n-1 \end{cases}$$

Note such z^* satisfies all constraints in the original constraint set when $\beta > 1$. Therefore when $\beta > 1$, the original constraint is strictly feasible. \square

Lemma A.2. *The below constraint set is strictly feasible only when $\beta > 1$.*

$$\begin{cases} |z^T|x - 1x_i| - 1^T \text{sign}(x - 1x_i)| \leq \beta \\ |z^T|x - 1x_i| + 1^T \text{sign}(-x + 1x_i)| \leq \beta \\ z^T \mathbf{1} = 0 \end{cases} \quad \forall i = 1, \dots, n$$

Proof. Consider without loss of generality that $x_1 < x_2 < \dots < x_n$. Then taking $i = 1$ and n in the first constraint gives $|z^T x - n| \leq \beta$ and $|z^T x - n + 2| \leq \beta$. It's necessary to have $\beta > 1$ and $z^T x = n - 1$ to have both constraints strictly satisfiable. Since we can always find z^* satisfying the below linear system

$$\begin{cases} x^T z^* = n - 1 \\ 1^T z^* = 0 \\ |x - 1x_i|^T z^* - 1^T \text{sign}(x - 1x_i) = -1 \quad \forall i = 2, \dots, n-1 \end{cases}$$

Note such z^* also satisfies

$$||-x + 1x_i|^T z^* + 1^T \text{sign}(-x + 1x_i)| \leq 1$$

Therefore when $\beta > 1$, the original constraint set is strictly feasible. \square

Lemma A.3. *The below constraint set is strictly feasible only when $\beta > 2$.*

$$\begin{cases} |z^T|x - 1x_i| - 1^T \text{sign}(x - 1x_i)| \leq \beta \\ |z^T|x - 1x_i| + 1^T \text{sign}(-x + 1x_i)| \leq \beta \\ z^T \mathbf{1} = 0 \\ z^T x = n \end{cases} \quad \forall i = 1, \dots, n$$

Proof. Consider without loss of generality that $x_1 < x_2 < \dots < x_n$. Then taking $i = n$ in the first constraint gives $|-n + (n-2)| \leq \beta$, which indicates that $\beta > 2$ is necessary for the constraint set to be strictly feasible. Since we can

always find z^* satisfying

$$\begin{cases} x^T z^* = n \\ 1^T z^* = 0 \\ |x - 1x_i|^T z^* - 1^T \text{sign}(x - 1x_i) = 0 \quad \forall i = 2, \dots, n-1 \end{cases}$$

Note such z^* also satisfies

$$\| -x + 1x_i \|^T z^* + 1^T \text{sign}(-x + 1x_i) \leq 2$$

Therefore when $\beta > 2$, the original constraint set is strictly feasible. \square

A.2. Proof of Theory 3.1 for ReLU Activation

Proof. Consider data $x \in \mathbb{R}^n$. Let m denote number of hidden neurons, then we have first layer weight $w \in \mathbb{R}^m$, first layer bias $b \in \mathbb{R}^m$, second layer weight $\alpha \in \mathbb{R}^m$ and second layer bias $b_0 \in \mathbb{R}$. The score matching objective is reduced to

$$p^* = \min_{w, \alpha, b} \frac{1}{2} \left\| \sum_{j=1}^m (xw_j + 1b_j)_+ \alpha_j + 1b_0 \right\|_2^2 + 1^T \left(\sum_{j=1}^m w_j \alpha_j \mathbb{1}\{xw_j + 1b_j \geq 0\} \right) + \frac{1}{2} \beta \sum_{j=1}^m (w_j^2 + \alpha_j^2).$$

According to Lemma 2 in (Pilanci & Ergen, 2020), after rescaling, the above problem is equivalent to

$$\min_{\substack{w, \alpha, b \\ |w_j|=1}} \frac{1}{2} \left\| \sum_{j=1}^m (xw_j + 1b_j)_+ \alpha_j + 1b_0 \right\|_2^2 + 1^T \left(\sum_{j=1}^m w_j \alpha_j \mathbb{1}\{xw_j + 1b_j \geq 0\} \right) + \beta \sum_{j=1}^m |\alpha_j|,$$

which can be written as

$$\begin{aligned} \min_{\substack{w, \alpha, b, r_1, r_2 \\ |w_j|=1}} & \frac{1}{2} \|r_1\|_2^2 + 1^T r_2 + \beta \sum_{j=1}^m |\alpha_j| \\ \text{s.t. } & r_1 = \sum_{j=1}^m (xw_j + 1b_j)_+ \alpha_j + 1b_0 \\ & r_2 = \sum_{j=1}^m w_j \alpha_j \mathbb{1}\{xw_j + 1b_j \geq 0\}. \end{aligned}$$

The dual problem writes

$$\begin{aligned} d^* = \max_{z_1, z_2} \min_{\substack{w, \alpha, b, r_1, r_2 \\ |w_j|=1}} & \frac{1}{2} \|r_1\|_2^2 + 1^T r_2 + \beta \sum_{j=1}^m |\alpha_j| + z_1^T \left(r_1 - \sum_{j=1}^m (xw_j + 1b_j)_+ \alpha_j - 1b_0 \right) \\ & + z_2^T \left(r_2 - \sum_{j=1}^m w_j \alpha_j \mathbb{1}\{xw_j + 1b_j \geq 0\} \right), \end{aligned}$$

which gives a lower bound of p^* . Minimizing over r_1, r_2, α_j above gives

$$\begin{aligned} \max_z \min_{b_0} & -\frac{1}{2} \|z\|_2^2 - b_0 z^T 1 \\ \text{s.t. } & |z^T (xw_j + 1b_j)_+ - w_j 1^T \mathbb{1}\{xw_j + 1b_j \geq 0\}| \leq \beta, \quad \forall |W_j| = 1, \forall b_j. \end{aligned}$$

For the constraints to hold, we must have $z^T \mathbf{1} = 0$ and b_j takes values over x_j 's. The above is equivalent to

$$\begin{aligned} & \max_z -\frac{1}{2} \|z\|_2^2 \\ & \text{s.t.} \begin{cases} |z^T(x - 1x_i)_+ - 1^T \mathbb{1}\{x - 1x_i \geq 0\}| \leq \beta \\ |z^T(x - 1x_i)_+ - 1^T \mathbb{1}\{x - 1x_i > 0\}| \leq \beta \\ |z^T(-x + 1x_i)_+ + 1^T \mathbb{1}\{-x + 1x_i \geq 0\}| \leq \beta \\ |z^T(-x + 1x_i)_+ + 1^T \mathbb{1}\{-x + 1x_i > 0\}| \leq \beta \\ z^T \mathbf{1} = 0 \end{cases} \quad \forall i = 1, \dots, n, \end{aligned} \quad (12)$$

According to Lemma A.1, when $\beta \geq 1$, the constraints in (12) are feasible for affine constraints, thus Slater's condition holds and the dual problem writes

$$\begin{aligned} d^* = & \min_{\substack{z_0, \dots, z_7, z_8 \\ \text{s.t. } z_0, \dots, z_7 \geq 0}} \max_z -\frac{1}{2} \|z\|_2^2 + \sum_{i=1}^n z_{0i} (z^T(x - 1x_i)_+ - 1^T \mathbb{1}\{x - 1x_i \geq 0\} + \beta) \\ & + \sum_{i=1}^n z_{1i} (-z^T(x - 1x_i)_+ + 1^T \mathbb{1}\{x - 1x_i \geq 0\} + \beta) + \sum_{i=1}^n z_{2i} (z^T(x - 1x_i)_+ - 1^T \mathbb{1}\{x - 1x_i > 0\} + \beta) \\ & + \sum_{i=1}^n z_{3i} (-z^T(x - 1x_i)_+ + 1^T \mathbb{1}\{x - 1x_i > 0\} + \beta) + \sum_{i=1}^n z_{4i} (z^T(-x + 1x_i)_+ + 1^T \mathbb{1}\{-x + 1x_i \geq 0\} + \beta) \\ & + \sum_{i=1}^n z_{5i} (-z^T(-x + 1x_i)_+ - 1^T \mathbb{1}\{-x + 1x_i \geq 0\} + \beta) + \sum_{i=1}^n z_{6i} (z^T(-x + 1x_i)_+ + 1^T \mathbb{1}\{-x + 1x_i > 0\} + \beta) \\ & + \sum_{i=1}^n z_{7i} (-z^T(-x + 1x_i)_+ - 1^T \mathbb{1}\{-x + 1x_i > 0\} + \beta) + z_8 z^T \mathbf{1}, \end{aligned}$$

which is equivalent to

$$\min_{\substack{z_0, \dots, z_7, z_8 \\ \text{s.t. } z_0, \dots, z_7 \geq 0}} \max_z -\frac{1}{2} \|z\|_2^2 + e^T z + f,$$

where

$$\begin{aligned} e = & \sum_{i=1}^n z_{0i}(x - 1x_i)_+ - \sum_{i=1}^n z_{1i}(x - 1x_i)_+ + \sum_{i=1}^n z_{2i}(x - 1x_i)_+ - \sum_{i=1}^n z_{3i}(x - 1x_i)_+ + \sum_{i=1}^n z_{4i}(-x + 1x_i)_+ \\ & - \sum_{i=1}^n z_{5i}(-x + 1x_i)_+ + \sum_{i=1}^n z_{6i}(-x + 1x_i)_+ - \sum_{i=1}^n z_{7i}(-x + 1x_i)_+ + 1z_8, \end{aligned}$$

and

$$\begin{aligned} f = & -\sum_{i=1}^n z_{0i} 1^T \mathbb{1}\{x - 1x_i \geq 0\} + \sum_{i=1}^n z_{1i} 1^T \mathbb{1}\{x - 1x_i \geq 0\} - \sum_{i=1}^n z_{2i} 1^T \mathbb{1}\{x - 1x_i > 0\} \\ & + \sum_{i=1}^n z_{3i} 1^T \mathbb{1}\{x - 1x_i > 0\} + \sum_{i=1}^n z_{4i} 1^T \mathbb{1}\{-x + 1x_i \geq 0\} - \sum_{i=1}^n z_{5i} 1^T \mathbb{1}\{-x + 1x_i \geq 0\} \\ & + \sum_{i=1}^n z_{6i} 1^T \mathbb{1}\{-x + 1x_i > 0\} - \sum_{i=1}^n z_{7i} 1^T \mathbb{1}\{-x + 1x_i > 0\} + \beta \left(\sum_{i=0}^7 \|z_i\|_1 \right). \end{aligned}$$

Maximizing over z gives

$$\min_{\substack{z_0, \dots, z_7, z_8 \\ \text{s.t. } z_0, \dots, z_7 \geq 0}} \frac{1}{2} \|e\|_2^2 + f,$$

Simplifying to get

$$\begin{aligned} & \min_{y_0, y_1, y_2, y_3, y_4} \frac{1}{2} \|A_1(y_0 + y_1) + A_2(y_2 + y_3) + 1y_4\|_2^2 + 1^T C_1 y_0 - 1^T C_3 y_2 \\ & + 1^T C_2 y_1 - 1^T C_4 y_3 + \beta (\|y_0\|_1 + \|y_1\|_1 + \|y_2\|_1 + \|y_3\|_1). \end{aligned}$$

Minimizing over y_4 gives the convex program (4) in Theorem 3.1 with $A = [\bar{A}_1, \bar{A}_1, \bar{A}_2, \bar{A}_2] \in \mathbb{R}^{n \times 4n}$, $b = [1^T C_1, 1^T C_2, -1^T C_3, -1^T C_4]^T \in \mathbb{R}^{4n}$ where $\bar{A}_1 = (I - \frac{1}{n} 11^T) A_1$, $\bar{A}_2 = (I - \frac{1}{n} 11^T) A_2$ with $[A_1]_{ij} = (x_i - x_j)_+$ and $[A_2]_{ij} = (-x_i + x_j)_+$, $[C_1]_{ij} = \mathbb{1}\{x_i - x_j \geq 0\}$, $[C_2]_{ij} = \mathbb{1}\{x_i - x_j > 0\}$, $[C_3]_{ij} = \mathbb{1}\{-x_i + x_j \geq 0\}$, $[C_4]_{ij} = \mathbb{1}\{-x_i + x_j > 0\}$. Once we obtain optimal solution y^* to problem (4), we can take

$$\begin{cases} w_j^* = \sqrt{|y_j^*|}, \alpha_j^* = \sqrt{|y_j^*|}, b_j^* = -\sqrt{|y_j^*|} x_j \text{ for } j = 1, \dots, n, \\ w_j^* = \sqrt{|y_j^*|}, \alpha_j^* = \sqrt{|y_j^*|}, b_j^* = -\sqrt{|y_j^*|} (x_{j-n} + \epsilon) \text{ for } j = n+1, \dots, 2n, \\ w_j^* = -\sqrt{|y_j^*|}, \alpha_j^* = \sqrt{|y_j^*|}, b_j^* = \sqrt{|y_j^*|} x_{j-2n} \text{ for } j = 2n+1, \dots, 3n, \\ w_j^* = -\sqrt{|y_j^*|}, \alpha_j^* = \sqrt{|y_j^*|}, b_j^* = \sqrt{|y_j^*|} (x_{j-3n} - \epsilon) \text{ for } j = 3n+1, \dots, 4n, \\ b_0^* = -\frac{1}{n} 1^T ([A_1, A_1, A_2, A_2] y^*), \end{cases} \quad (13)$$

then score matching objective has the same value as optimal value of convex program (4) as $\epsilon \rightarrow 0$, which indicates $p^* = d^*$ and the above parameter set is optimal. \square

A.3. Convex Programs for Univariate Data with More Model Architectures

A.3.1. ABSOLUTE ACTIVATION WITHOUT SKIP CONNECTION

Theorem A.4. *When σ is absolute value activation and $V = 0$, denote the optimal score matching objective value (2) with s_θ specified in (3) as p^* , when $m \geq m^*$ and $\beta \geq 1$,*

$$p^* = \min_y \frac{1}{2} \|Ay\|_2^2 + b^T y + \beta \|y\|_1, \quad (14)$$

where $m^* = \|y^*\|_0$, and y^* is any optimal solution to (14). A, b and reconstruction rule for θ is specified in the proof below.

Proof. Consider data $x \in \mathbb{R}^n$. Let m denote number of hidden neurons, then we have first layer weight $w \in \mathbb{R}^m$, first layer bias $b \in \mathbb{R}^m$, second layer weight $\alpha \in \mathbb{R}^m$ and second layer bias $b_0 \in \mathbb{R}$. Then the score matching objective is reduced to

$$p^* = \min_{w, \alpha, b} \frac{1}{2} \left\| \sum_{j=1}^m |xw_j + 1b_j| \alpha_j + 1b_0 \right\|_2^2 + 1^T \left(\sum_{j=1}^m w_j \alpha_j \text{sign}(xw_j + 1b_j) \right) + \frac{1}{2} \beta \sum_{j=1}^m (w_j^2 + \alpha_j^2).$$

According to Lemma 2 in (Pilanci & Ergen, 2020), after rescaling, the above problem is equivalent to

$$\min_{\substack{w, \alpha, b \\ |w_j|=1}} \frac{1}{2} \left\| \sum_{j=1}^m |xw_j + 1b_j| \alpha_j + 1b_0 \right\|_2^2 + 1^T \left(\sum_{j=1}^m w_j \alpha_j \text{sign}(xw_j + 1b_j) \right) + \beta \sum_{j=1}^m |\alpha_j|,$$

which can be written as

$$\begin{aligned} \min_{\substack{w, \alpha, b, r_1, r_2 \\ |w_j|=1}} & \frac{1}{2} \|r_1\|_2^2 + 1^T r_2 + \beta \sum_{j=1}^m |\alpha_j| \\ \text{s.t.} & r_1 = \sum_{j=1}^m |xw_j + 1b_j| \alpha_j + 1b_0 \\ & r_2 = \sum_{j=1}^m w_j \alpha_j \text{sign}(xw_j + 1b_j). \end{aligned} \quad (15)$$

The dual problem of (15) writes

$$\begin{aligned} d^* = \max_{z_1, z_2} \min_{\substack{w, \alpha, b, r_1, r_2 \\ |w_j|=1}} & \frac{1}{2} \|r_1\|_2^2 + 1^T r_2 + \beta \sum_{j=1}^m |\alpha_j| + z_1^T \left(r_1 - \sum_{j=1}^m |xw_j + 1b_j| \alpha_j - 1b_0 \right) \\ & + z_2^T \left(r_2 - \sum_{j=1}^m w_j \alpha_j \text{sign}(xw_j + 1b_j) \right), \end{aligned}$$

which is a lower bound of optimal value to the original problem, i.e., $p^* \geq d^*$. Minimizing over r_1 and r_2 gives

$$\max_z \min_{\substack{w, \alpha, b \\ |w_j|=1}} -\frac{1}{2} \|z\|_2^2 + \beta \sum_{j=1}^m |\alpha_j| - z^T \left(\sum_{j=1}^m |xw_j + 1b_j| \alpha_j + 1b_0 \right) + 1^T \sum_{j=1}^m w_j \alpha_j \text{sign}(xw_j + 1b_j).$$

Minimizing over α_j gives

$$\begin{aligned} \max_z \min_{b_0} -\frac{1}{2} \|z\|_2^2 - b_0 z^T \mathbf{1} \\ \text{s.t. } |z^T |xw_j + 1b_j| - w_j 1^T \text{sign}(xw_j + 1b_j)| \leq \beta, \quad \forall |w_j| = 1, \forall b_j, \end{aligned}$$

which is equivalent to

$$\begin{aligned} \max_z \min_{b_0} -\frac{1}{2} \|z\|_2^2 - b_0 z^T \mathbf{1} \\ \text{s.t. } \begin{cases} |z^T |x + 1b_j| - 1^T \text{sign}(x + 1b_j)| \leq \beta \\ |z^T | - x + 1b_j| + 1^T \text{sign}(-x + 1b_j)| \leq \beta \end{cases} \quad \forall b_j. \end{aligned}$$

For the constraints to hold, we must have $z^T \mathbf{1} = 0$ and b_j takes values over x_j 's. Furthermore, since sign is discontinuous at input 0, we add another function sign^* which takes value -1 at input 0 to cater for the constraints. The above is equivalent to

$$\begin{aligned} \max_z -\frac{1}{2} \|z\|_2^2 \\ \text{s.t. } \begin{cases} |z^T |x - 1x_i| - 1^T \text{sign}(x - 1x_i)| \leq \beta \\ |z^T |x - 1x_i| - 1^T \text{sign}^*(x - 1x_i)| \leq \beta \\ |z^T | - x + 1x_i| + 1^T \text{sign}(-x + 1x_i)| \leq \beta \\ |z^T | - x + 1x_i| + 1^T \text{sign}^*(-x + 1x_i)| \leq \beta \\ z^T \mathbf{1} = 0 \end{cases} \quad \forall i = 1, \dots, n. \end{aligned} \quad (16)$$

Since the second constraint overlaps with the third, and the fourth constraint overlaps with the first, (16) is equivalent to

$$\begin{aligned} \max_z -\frac{1}{2} \|z\|_2^2 \\ \text{s.t. } \begin{cases} |z^T |x - 1x_i| - 1^T \text{sign}(x - 1x_i)| \leq \beta \\ |z^T | - x + 1x_i| + 1^T \text{sign}(-x + 1x_i)| \leq \beta \\ z^T \mathbf{1} = 0 \end{cases} \quad \forall i = 1, \dots, n. \end{aligned} \quad (17)$$

According to Lemma A.2, when $\beta \geq 1$, the constraints in (17) are feasible for affine constraints, thus Slater's condition holds and the dual problem writes

$$\begin{aligned} d^* = \min_{\substack{z_0, z_1, z_2, z_3, z_4 \\ \text{s.t. } z_0, z_1, z_2, z_3 \geq 0}} \max_z -\frac{1}{2} \|z\|_2^2 + \sum_{i=1}^n z_{0i} (z^T |x - 1x_i| - 1^T \text{sign}(x - 1x_i) + \beta) \\ + \sum_{i=1}^n z_{1i} (-z^T |x - 1x_i| + 1^T \text{sign}(x - 1x_i) + \beta) \\ + \sum_{i=1}^n z_{2i} (z^T | - x + 1x_i| + 1^T \text{sign}(-x + 1x_i) + \beta) \\ + \sum_{i=1}^n z_{3i} (-z^T | - x + 1x_i| - 1^T \text{sign}(-x + 1x_i) + \beta) \\ + z_4 z^T \mathbf{1}, \end{aligned}$$

which is equivalent to

$$\min_{\substack{z_0, z_1, z_2, z_3, z_4 \\ \text{s.t. } z_0, z_1, z_2, z_3 \geq 0}} \max_z -\frac{1}{2} \|z\|_2^2 + e^T z + f,$$

where

$$e = \sum_{i=1}^n z_{0i}|x - 1x_i| - \sum_{i=1}^n z_{1i}|x - 1x_i| + \sum_{i=1}^n z_{2i}| -x + 1x_i| - \sum_{i=1}^n z_{3i}| -x + 1x_i| + 1z_4$$

and

$$f = - \sum_{i=1}^n z_{0i}1^T \text{sign}(x - 1x_i) + \sum_{i=1}^n z_{1i}1^T \text{sign}(x - 1x_i) + \sum_{i=1}^n z_{2i}1^T \text{sign}(-x + 1x_i) - \sum_{i=1}^n z_{3i}1^T \text{sign}(-x + 1x_i) + \beta(\|z_0\|_1 + \|z_1\|_1 + \|z_2\|_1 + \|z_3\|_1).$$

Maximizing over z gives

$$\min_{z_0, z_1, z_2, z_3, z_4} \frac{1}{2} \|e\|_2^2 + f. \\ \text{s.t. } z_0, z_1, z_2, z_3 \geq 0$$

Simplifying to get

$$\min_{y_1, y_2, z} \frac{1}{2} \|A_1(y_1 + y_2) + 1z\|_2^2 + 1^T C_1 y_1 - 1^T C_2 y_2 + \beta(\|y_1\|_1 + \|y_2\|_1).$$

Minimizing over z gives the convex program (14) in Theorem A.4 where $A = [\bar{A}_1, \bar{A}_1] \in \mathbb{R}^{n \times 2n}$, $b = [1^T C_1, -1^T C_2]^T \in \mathbb{R}^{2n}$ with $\bar{A}_1 = (I - \frac{1}{n}11^T) A_1$, $[A_1]_{ij} = |x_i - x_j|$, $[C_1]_{ij} = \text{sign}(x_i - x_j)$ and $[C_2]_{ij} = \text{sign}(-x_i + x_j)$. Once we obtain optimal solution y^* to problem (14), we can take

$$\begin{cases} w_j^* = \sqrt{|y_j^*|}, \alpha_j^* = \sqrt{|y_j^*|}, b_j^* = -\sqrt{|y_j^*|}x_j \text{ for } j = 1, \dots, n, \\ w_j^* = -\sqrt{|y_j^*|}, \alpha_j^* = \sqrt{|y_j^*|}, b_j^* = \sqrt{|y_j^*|}x_{j-n} \text{ for } j = n + 1, \dots, 2n, \\ b_0^* = -\frac{1}{n}1^T([A_1, A_1]y^*), \end{cases}$$

then score matching objective has the same value as optimal value of convex program (14), which indicates $p^* = d^*$ and the above parameter set is optimal. \square

A.3.2. SCORE FUNCTIONS FOR GAUSSIAN AND GAUSSIAN MIXTURE DISTRIBUTIONS

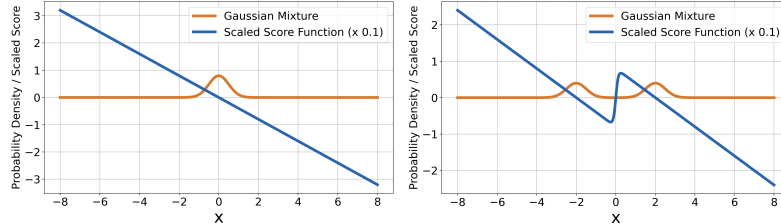


Figure 6. Probability densities and score functions for Gaussian distribution and Gaussian mixture distribution with two components. Here we scale the score function with 0.1 for better visibility.

A.3.3. RELU ACTIVATION WITH SKIP CONNECTION

Theorem A.5. When σ is ReLU and $V \neq 0$, denote the optimal score matching objective value (2) with s_θ specified in (3) as p^* , when $m \geq m^*$ and $\beta \geq 1$,

$$p^* = \min_y \frac{1}{2} \|Ay\|_2^2 + b^T y + c + 2\beta \|y\|_1, \quad (18)$$

where $m^* = \|y^*\|_0$, and y^* is any optimal solution to (18). A, b, c and reconstruction rule for θ is specified in the proof below.

Proof. Here we reduce score matching objective including ReLU activation to score matching objective including absolute value activation and exploits results in Theorem A.6. Let $\{w^r, b^r, \alpha^r, v^r\}$ denotes parameter set corresponding to ReLU activation, consider another parameter set $\{w^a, b^a, \alpha^a, v^a\}$ satisfying

$$\begin{cases} \alpha^r = 2\alpha^a, \\ w^r = w^a, \\ b^r = b^a, \\ b_0^r = b_0^a - \frac{1}{2} \sum_{j=1}^m b_j^r \alpha_j^r, \\ v^r = v^a - \frac{1}{2} \sum_{j=1}^m w_j^r \alpha_j^r. \end{cases}$$

Then the score matching objective

$$\min_{w^r, \alpha^r, b^r, v^r} \frac{1}{2} \left\| \sum_{j=1}^m (xw_j^r + 1b_j^r)_+ \alpha_j^r + xv^r + 1b_0^r \right\|_2^2 + 1^T \left(\sum_{j=1}^m w_j^r \alpha_j^r \mathbb{1}\{xw_j^r + 1b_j^r \geq 0\} \right) + nv^r + \frac{\beta}{2} \sum_{j=1}^m (w_j^{r2} + \alpha_j^{r2})$$

is equivalent to

$$\min_{w^a, \alpha^a, b^a, v^a} \frac{1}{2} \left\| \sum_{j=1}^m |xw_j^a + 1b_j^a| \alpha_j^a + xv^a + 1b_0^a \right\|_2^2 + 1^T \left(\sum_{j=1}^m w_j^a \alpha_j^a \text{sign}(xw_j^a + 1b_j^a) \right) + nv^a + \frac{\beta}{2} \sum_{j=1}^m (w_j^{a2} + 4\alpha_j^{a2}).$$

According to Lemma 2 in (Pilanci & Ergen, 2020), after rescaling, the above problem is equivalent to

$$\min_{\substack{w^a, \alpha^a, b^a, v^a \\ |w_j^a|=1}} \frac{1}{2} \left\| \sum_{j=1}^m |xw_j^a + 1b_j^a| \alpha_j^a + xv^a + 1b_0^a \right\|_2^2 + 1^T \left(\sum_{j=1}^m w_j^a \alpha_j^a \text{sign}(xw_j^a + 1b_j^a) \right) + nv^a + 2\beta \sum_{j=1}^m |\alpha_j^a|. \quad (19)$$

Following similar analysis as in Appendix A.3.4 with a different rescaling factor we can derive the convex program (18) with $A = B^{\frac{1}{2}} A_1$, $b = A_1^T (-n\bar{x}/\|\bar{x}\|_2^2) + b_1$, $c = -n^2/(2\|\bar{x}\|_2^2)$ where $B = I - P_{\bar{x}}$ with $P_{\bar{x}} = \bar{x}\bar{x}^T/\|\bar{x}\|_2^2$, and A_1, b_1 are identical to A, b defined in Section A.3.1 respectively. Here, $\bar{x}_j := x_j - \sum_i x_i/n$ denotes mean-subtracted data vector. The optimal solution set to (19) is given by

$$\begin{cases} w_j^{a*} = \sqrt{2|y_j^*|}, \alpha_j^{a*} = \sqrt{|y_j^*|/2}, b_j^{a*} = -\sqrt{2|y_j^*|}x_j \text{ for } j = 1, \dots, n, \\ W_j^{a*} = -\sqrt{2|y_j^*|}, \alpha_j^{a*} = \sqrt{|y_j^*|/2}, b_j^{a*} = \sqrt{2|y_j^*|}x_{j-n} \text{ for } j = n+1, \dots, 2n, \\ v^{a*} = -(\bar{x}^T A_1 y^* + n)/\|\bar{x}\|_2^2, \\ b_0^{a*} = -\frac{1}{n} 1^T ([A_1', A_1'] y^* + xv^{a*}), \end{cases}$$

where A_1' is A_1 defined in Appendix A.3.1 and y^* is optimal solution to convex program (18). Then the optimal parameter set $\{w^r, b^r, \alpha^r, z^r\}$ is given by

$$\begin{cases} w_j^{r*} = \sqrt{2|y_j^*|}, \alpha_j^{r*} = \sqrt{2|y_j^*|}, b_j^{r*} = -\sqrt{2|y_j^*|}x_j \text{ for } j = 1, \dots, n, \\ w_j^{r*} = -\sqrt{2|y_j^*|}, \alpha_j^{r*} = \sqrt{2|y_j^*|}, b_j^{r*} = \sqrt{2|y_j^*|}x_{j-n} \text{ for } j = n+1, \dots, 2n, \\ v^{r*} = -(\bar{x}^T A_1 y^* + n)/\|\bar{x}\|_2^2 - \sum_{j=1}^m w_j^{r*} \alpha_j^{r*}/2, \\ b_0^{r*} = -\frac{1}{n} 1^T ([A_1', A_1'] y^* + x(-\bar{x}^T A_1 y^* + n)/\|\bar{x}\|_2^2) - \sum_{j=1}^m b_j^{r*} \alpha_j^{r*}/2. \end{cases}$$

□

A.3.4. ABSOLUTE VALUE ACTIVATION WITH SKIP CONNECTION

Theorem A.6. When σ is absolute value activation and $V \neq 0$, denote the optimal score matching objective value (2) with σ_θ specified in (3) as p^* , when $m \geq m^*$ and $\beta \geq 2$,

$$p^* = \min_y \frac{1}{2} \|Ay\|_2^2 + b^T y + \beta \|y\|_1, \quad (20)$$

where $m^* = \|y^*\|_0$, and y^* is any optimal solution to (20). A, b and reconstruction rule for θ is specified in the proof below.

Proof. Consider data matrix $x \in \mathbb{R}^n$, then the score matching objective is reduced to

$$p^* = \min_{w, \alpha, b, v} \frac{1}{2} \left\| \sum_{j=1}^m |xw_j + 1b_j| \alpha_j + xv + 1b_0 \right\|_2^2 + 1^T \left(\sum_{j=1}^m w_j \alpha_j \text{sign}(xw_j + 1b_j) \right) + nv + \frac{1}{2} \beta \sum_{j=1}^m (w_j^2 + \alpha_j^2).$$

Following similar analysis as in Appendix A.3.1, we can derive the dual problem as

$$d^* = \max_{z_1, z_2} \min_{w, \alpha, b, v, r_1, r_2} \frac{1}{2} \|r_1\|_2^2 + 1^T r_2 + nv + \beta \sum_{j=1}^m |\alpha_j| + z_1^T \left(r_1 - \sum_{j=1}^m |xw_j + 1b_j| \alpha_j - xv - 1b_0 \right) + z_2^T \left(r_2 - \sum_{j=1}^m w_j \alpha_j \text{sign}(xw_j + 1b_j) \right).$$

which gives a lower bound of p^* . Minimizing over r_1 and r_2 gives

$$\max_{z_1} \min_{w, \alpha, b, v} -\frac{1}{2} \|z_1\|_2^2 + nv + \beta \sum_{j=1}^m |\alpha_j| - z_1^T \left(\sum_{j=1}^m |xw_j + 1b_j| \alpha_j + xv + 1b_0 \right) + 1^T \sum_{j=1}^m w_j \alpha_j \text{sign}(xw_j + 1b_j).$$

Minimizing over v gives

$$\max_{z_1} \min_{w, \alpha, b} -\frac{1}{2} \|z_1\|_2^2 + \beta \sum_{j=1}^m |\alpha_j| - z_1^T \left(\sum_{j=1}^m |xw_j + 1b_j| \alpha_j + 1b_0 \right) + 1^T \sum_{j=1}^m w_j \alpha_j \text{sign}(xw_j + 1b_j).$$

Minimizing over α_j gives

$$\max_z \min_{b_0} -\frac{1}{2} \|z\|_2^2 - b_0 z^T \mathbf{1}$$

$$\text{s.t. } \begin{cases} z^T x = n \\ |z^T |xw_j + 1b_j| - w_j \mathbf{1}^T \text{sign}(xw_j + 1b_j)| \leq \beta, \quad \forall |w_j| = 1, \forall b_j. \end{cases}$$

Following same logic as in Appendix A.3.1, the above problem is equivalent to

$$\max_z -\frac{1}{2} \|z\|_2^2$$

$$\text{s.t. } \begin{cases} |z^T |x - 1x_i| - \mathbf{1}^T \text{sign}(x - 1x_i)| \leq \beta \\ |z^T | - x + 1x_i| + \mathbf{1}^T \text{sign}(-x + 1x_i)| \leq \beta \\ z^T \mathbf{1} = 0 \\ z^T x = n \end{cases} \quad \forall i = 1, \dots, n. \quad (21)$$

According to Lemma A.3, when $\beta \geq 2$, the constraints in (21) are feasible for affine constraints, thus Slater's condition

holds and the dual problem writes

$$\begin{aligned}
 d^* = \min_{\substack{z_0, z_1, z_2, z_3, z_4, z_5 \\ \text{s.t. } z_0, z_1, z_2, z_3 \geq 0}} \max_z & -\frac{1}{2} \|z\|_2^2 + \sum_{i=1}^n z_{0i} (z^T |x - 1x_i| - 1^T \text{sign}(x - 1x_i) + \beta) \\
 & + \sum_{i=1}^n z_{1i} (-z^T |x - 1x_i| + 1^T \text{sign}(x - 1x_i) + \beta) \\
 & + \sum_{i=1}^n z_{2i} (z^T |-x + 1x_i| + 1^T \text{sign}(-x + 1x_i) + \beta) \\
 & + \sum_{i=1}^n z_{3i} (-z^T |-x + 1x_i| - 1^T \text{sign}(-x + 1x_i) + \beta) \\
 & + z_4(z^T x - n) + z_5 z^T \mathbf{1},
 \end{aligned}$$

which is equivalent to

$$\min_{\substack{z_0, z_1, z_2, z_3, z_4, z_5 \\ \text{s.t. } z_0, z_1, z_2, z_3 \geq 0}} \max_z -\frac{1}{2} \|z\|_2^2 + e^T z + f,$$

where

$$e = \sum_{i=1}^n z_{0i} |x - 1x_i| - \sum_{i=1}^n z_{1i} |x - 1x_i| + \sum_{i=1}^n z_{2i} |-x + 1x_i| - \sum_{i=1}^n z_{3i} |-x + 1x_i| + xz_4 + 1z_5,$$

and

$$\begin{aligned}
 f = & -\sum_{i=1}^n z_{0i} 1^T \text{sign}(x - 1x_i) + \sum_{i=1}^n z_{1i} 1^T \text{sign}(x - 1x_i) + \sum_{i=1}^n z_{2i} 1^T \text{sign}(-x + 1x_i) \\
 & - \sum_{i=1}^n z_{3i} 1^T \text{sign}(-x + 1x_i) - z_4 n + \beta(\|z_0\|_1 + \|z_1\|_1 + \|z_2\|_1 + \|z_3\|_1).
 \end{aligned}$$

Maximizing over z gives

$$\min_{\substack{z_0, z_1, z_2, z_3, z_4, z_5 \\ \text{s.t. } z_0, z_1, z_2, z_3 \geq 0}} \frac{1}{2} \|e\|_2^2 + f.$$

Simplifying to get

$$\min_{y_0, y_1, y_2, y_3} \frac{1}{2} \|A'_1(y_0 + y_1) + xy_2 + 1y_3\|_2^2 + 1^T C_1 y_0 - 1^T C_2 y_1 + ny_2 + \beta(\|y_1\|_1 + \|y_2\|_1), \quad (22)$$

where A'_1, C_1, C_2 are as A_1, C_1, C_2 defined in Appendix A.3.1. Minimizing over y_3 gives $y_3 = -1^T(A'_1(y_0 + y_1) + xy_2)/n$ and (22) is reduced to

$$\min_{y_0, y_1, y_2} \frac{1}{2} \|\bar{A}'_1(y_0 + y_1) + \bar{x}y_2\|_2^2 + 1^T C_1 y_0 - 1^T C_2 y_1 + ny_2 + \beta(\|y_1\|_1 + \|y_2\|_1),$$

where \bar{A}'_1 is as \bar{A}_1 defined in Appendix A.3.1. Minimizing over y_2 gives $y_2 = -(\bar{x}^T \bar{A}'_1(y_0 + y_1) + n) / \|\bar{x}\|_2^2$ and the above problem is equivalent to the convex program (20) in Theorem A.6 with $A = B^{\frac{1}{2}} A_1, b = A_1^T (-n\bar{x} / \|\bar{x}\|_2^2) + b_1, c = -n^2 / (2\|\bar{x}\|_2^2)$ where $B = I - P_{\bar{x}}$ with $P_{\bar{x}} = \bar{x}\bar{x}^T / \|\bar{x}\|_2^2$, and A_1, b_1 are identical to A, b defined in Section A.3.1 respectively. Once we obtain optimal solution y^* to problem (20), we can take

$$\begin{cases} w_j^* = \sqrt{|y_j^*|}, \alpha_j^* = \sqrt{|y_j^*|}, b_j^* = -\sqrt{|y_j^*|} x_j \text{ for } j = 1, \dots, n, \\ w_j^* = -\sqrt{|y_j^*|}, \alpha_j^* = \sqrt{|y_j^*|}, b_j^* = \sqrt{|y_j^*|} x_{j-n} \text{ for } j = n+1, \dots, 2n, \\ v^* = -(\bar{x}^T A_1 y^* + n) / \|\bar{x}\|_2^2, \\ b_0^* = -\frac{1}{n} 1^T ([A'_1, A'_1] y^* + xv^*), \end{cases}$$

then score matching objective has the same value as optimal value of convex program (20), which indicates $p^* = d^*$ and the above parameter set is optimal. \square

A.4. Explanation for Unbounded Objective Value

Here we illustrate via a simple example that weight decay is necessary for the optimal objective value to stay finite. Follow notation in Appendix A.2, consider for example only one data point and one hidden neuron, then objective function for the neural network with ReLU activation and no skip connection would be

$$\frac{1}{2}((xw + b)_+ \alpha + b_0)^2 + w\alpha \mathbb{1}(xw + b \geq 0) + \frac{\beta}{2}(w^2 + \alpha^2).$$

WLOG consider $x = 1$, then when weight decay parameter $0 \leq \beta < 1$, set $b = -w + \sqrt{1 - \beta}$ and $b_0 = 0$ above, we get

$$\frac{1 - \beta}{2}\alpha^2 + w\alpha + \frac{\beta}{2}(w^2 + \alpha^2).$$

Then we can set $\alpha = -w$ and the above expression becomes $(\beta - 1)w^2/2$. Thus the objective goes to minus infinity when w goes to infinity.

A.5. Proof in Section 3.3

Proof. The optimality condition for convex program (4) is

$$0 \in A^T Ay + b + \beta \theta_1, \quad (23)$$

where $\theta_1 \in \partial \|y\|_1$. To show y^* satisfies optimality condition (23), let a_i denote the i th column of A . Check the first entry,

$$a_1^T Ay + b_1 + \beta(-1) = nv y_1^* - nv y_{3n}^* + n - \beta = 0.$$

Check the $3n$ th entry,

$$a_{3n}^T Ay + b_{3n} + \beta = -nv y_1^* + nv y_{3n}^* - n + \beta = 0.$$

For j th entry with $j \notin \{1, 3n\}$, note

$$\begin{aligned} & |a_j^T Ay + b_j| \\ &= |a_j^T (a_1 y_1^* + a_{3n} y_{3n}^*) + b_j| \\ &= |a_j^T (a_1 y_1^* - a_1 y_{3n}^*) + b_j| \\ &= \left| \frac{\beta - n}{nv} a_j^T a_1 + b_j \right|. \end{aligned}$$

Since $|b_j| \leq n - 1$, by continuity, $|a_j^T Ay + b_j| \leq \beta$ should hold as we decrease β a little further to threshold $\beta_1 = \max_{j \notin \{1, 3n\}} |a_j^T Ay + b_j|$. Therefore, y^* is optimal. \square

A.6. Supplementary Case Studies

A.6.1. ABSOLUTE VALUE ACTIVATION WITHOUT SKIP CONNECTION

In this section, we show that convex program (14) can be solved analytically for certain weight decay range and the predicted score function may not be compliant with log-concave sampling convergence theory. When $\beta > \|b\|_\infty$, $y = 0$ is optimal and the predicted score is always zero. When β is decreased further to some threshold $\beta_2 < n$, i.e., when $\beta_2 < \beta \leq n$, then

$$y = \left[\frac{\beta - n}{2nv} + t, \quad 0, \quad \dots, \quad 0, \quad \frac{n - \beta}{2nv} + t \right]^T$$

is optimal with any $t \in \mathbb{R}$ such that $|t| \leq \frac{n - \beta}{2nv}$ where μ and v denotes the sample mean and sample variance as described in Section 3.3⁵. For any test data \hat{x} , the corresponding predicted score \hat{y} is given by

$$\begin{cases} \hat{y} = \frac{\beta - n}{nv}(\hat{x} - \mu), & x_1 \leq \hat{x} \leq x_n \\ \hat{y} = -2t\hat{x} + \left(\frac{\beta - n}{nv} + 2t\right)x_1 + \frac{n - \beta}{nv}\mu, & \hat{x} < x_1 \\ \hat{y} = 2t\hat{x} - \left(\frac{n - \beta}{nv} + 2t\right)x_n + \frac{n - \beta}{nv}\mu. & \hat{x} > x_n \end{cases} \quad (24)$$

⁵See Appendix A.7.1 for proof and value of β_2 .

Theorem A.7. (Convergence Result) When s_θ is of two-layer neural network with absolute value activation and $\beta_2 < \beta \leq n$, let π^1 denote the target distribution (defined below). For any $\epsilon \in [0, 1]$, if we take step size $\eta \asymp \frac{\epsilon^2 nv}{n-\beta}$, then for the mixture distribution $\bar{\mu} = T^{-1} \sum_{t=1}^T x^t$, it holds that $\sqrt{KL(\bar{\mu} \parallel \pi^1)} \leq \epsilon$ after

$$O\left(\frac{(n-\beta)W_2^2(\mu_0, \pi^1)}{nv\epsilon^4}\right) \text{ iterations,}$$

where W_2 denotes 2-Wasserstein distance and π^1 satisfies

$$\pi^1 \propto \begin{cases} \exp\left(\frac{\beta-n}{nv}(x_1 - \mu)x + \frac{n-\beta}{2nv}x_1^2\right), & x < x_1, \\ \exp\left(\frac{\beta-n}{2nv}x^2 - \frac{\mu(\beta-n)}{nv}x\right), & x_1 \leq x \leq x_n, \\ \exp\left(\frac{\beta-n}{nv}(x_n - \mu)x + \frac{n-\beta}{2nv}x_n^2\right), & x \geq x_n. \end{cases}$$

Proof. See Appendix A.7.2. □

A.6.2. RELU WITH SKIP CONNECTION

In the convex program (18), $y = 0$ is an optimal solution when $2\beta \geq \|b\|_\infty$. Therefore, following the reconstruction procedure described in Appendix A.3.3, the corresponding neural network parameter set is given by $\{W^{(1)} = 0, b^{(1)} = 0, W^{(2)} = 0, b^{(2)} = \mu/v, V = -1/v\}$ with μ and v denotes the sample mean and sample variance as described in Section 3.3. For any test data \hat{x} , the corresponding predicted score is given by

$$\hat{y} = V\hat{x} + b^{(2)} = -\frac{1}{v}(\hat{x} - \mu),$$

which gives the score function of Gaussian distribution with mean being sample mean and variance being sample variance. Therefore, adding skip connection would change the zero score prediction to a linear function parameterized by sample mean and variance in the large weight decay regime.

A.6.3. ABSOLUTE VALUE ACTIVATION WITH SKIP CONNECTION

Consider convex program (20), when $\beta > \|b\|_\infty$, $y = 0$ is optimal. Following the reconstruction procedure described in Appendix B.2.3, the corresponding neural network parameter set is given by $\{W^{(1)} = 0, b^{(1)} = 0, W^{(2)} = 0, b^{(2)} = \mu/v, V = -1/v\}$ with μ and v denotes the sample mean and sample variance as described in Section 3.3. For any testing data \hat{x} , the corresponding predicted score is given by

$$\hat{y} = V\hat{x} + b^{(2)} = -\frac{1}{v}(\hat{x} - \mu),$$

which is the score function of Gaussian distribution with mean being sample mean and variance being sample variance, just as the case for σ being ReLU activation and $V \neq 0$ described in Appendix A.6.2.

A.7. Proof in Supplementary Case Study

A.7.1. PROOF FOR OPTIMALITY CONDITION

Proof. Assume without loss of generality data points are ordered as $x_1 < \dots < x_n$, then

$$b = [n, n-2, \dots, -(n-2), n-2, n-4, \dots, -n].$$

The optimality condition to the convex program (14) is given by

$$0 \in A^T A y + b + \beta \theta_1, \tag{25}$$

where $\theta_1 \in \partial \|y\|_1$. To show y^* satisfies optimality condition (25), let a_i denote the i th column of A . We check the first entry

$$a_1^T A y + b_1 + \beta(-1) = nv y_1 - nv y_n + n - \beta = 0.$$

We then check the last entry

$$a_n^T A y + b_n + \beta = -n v y_1 + n v y_n - n + \beta = 0.$$

For j th entry with $1 < j < n$, note

$$\begin{aligned} & |a_j^T A y + b_j| \\ &= |a_j^T (a_1 y_1 + a_n y_n) + b_j| \\ &= |a_j^T (a_1 y_1 - a_1 y_n) + b_j| \\ &= \left| \frac{\beta - n}{n v} a_j^T a_1 + b_j \right|. \end{aligned}$$

Since $|b_j| \leq n - 2$, by continuity, $|a_j^T A y + b_j| \leq \beta$ should hold as we decrease β a little further to some threshold $\beta_2 = \max_{j \notin \{1, n\}} |a_j^T A y + b_j|$. Therefore, y^* satisfies (25). \square

A.7.2. CONVERGENCE PROOF

Proof. When $\beta_2 < \beta \leq n$, the predicted score function is differentiable almost everywhere with least slope 0 and largest slope $(n - \beta)/(n v)$. Then since the integrated score function is weakly concave, Theorem A.7 follows case 1 in Theorem 4.3.6 in (Chewi, 2023). \square

A.8. Supplementary Definition and Proof for Section 3.4

Let $y_i^* \in \mathbb{R}^4$ with $[y_i^*]_j = y_{(j-1)n+i}^*$ and $[\mathcal{D}(x, x_i)] = [(x - x_i)_+, (x - x_i + \epsilon)_+, (-x + x_i)_+, (-x + x_i - \epsilon)_+]^T$ with $\epsilon \rightarrow 0$, b_0^* defined in (13). Now we proceed to prove the convergence result in Section 3.4.

A.8.1. CONVERGENCE PROOF

Proof. When $\beta_1 < \beta \leq n$, the predicted score function is differentiable almost everywhere with least slope 0 and largest slope $(n - \beta)/(n v)$. Then since the integrated score function is weakly concave, Theorem 3.4 follows case 1 in Theorem 4.3.6 in (Chewi, 2023). \square

A.9. Supplementary Assumption and Proof for Theorem 3.2

Assumption A.8. Assume the data matrix X induces no singular cone as defined in Proposition 3.1 in (Mishkin et al., 2022).

A.9.1. PROOF OF THEOREM 3.2

Proof. When $X \in \mathbb{R}^{n \times d}$ for some $d > 1$. Let m denote the number of hidden neurons, then the score matching objective can be reduced to

$$p^* = \min_{u_j, v_j} \sum_{i=1}^n \left(\frac{1}{2} \left\| \sum_{j=1}^m (X_i u_j)_+ v_j^T \right\|_2^2 + \text{tr} \left(\nabla_{X_i} \left[\sum_{j=1}^m (X_i u_j)_+ v_j^T \right] \right) \right), \quad (26)$$

which can be rewritten as

$$\min_{u_j, v_j} \frac{1}{2} \left\| \sum_{j=1}^m (X u_j)_+ v_j^T \right\|_F^2 + 1^T \left(\sum_{j=1}^m \mathbb{1}\{X u_j \geq 0\} v_j^T u_j \right). \quad (27)$$

Let $D'_j = \text{diag}(\mathbb{1}\{X u_j \geq 0\})$, then problem (27) is equivalent to

$$\min_{u_j, v_j} \frac{1}{2} \left\| \sum_{j=1}^m D'_j X u_j v_j^T \right\|_F^2 + \sum_{j=1}^m \text{tr}(D'_j) v_j^T u_j. \quad (28)$$

Thus

$$p^* = \min_{\substack{W_j = u_j v_j^T \\ (2D_j' - I)Xu_j \geq 0}} \frac{1}{2} \left\| \sum_{j=1}^m D_j' X W_j \right\|_F^2 + \sum_{j=1}^m \text{tr}(D_j') \text{tr}(W_j) \quad (29)$$

$$\geq \min_{W_j} \frac{1}{2} \left\| \sum_{j=1}^P D_j X W_j \right\|_F^2 + \sum_{j=1}^P \text{tr}(D_j) \text{tr}(W_j), \quad (30)$$

where D_1, \dots, D_P enumerates all possible sign patterns of $\text{diag}(\mathbb{1}\{Xu \geq 0\})$. To prove the reverse direction, let W_j^* be the optimal solution to the convex program (5), we provide a way to reconstruct optimal $\{u_j, v_j\}$ which achieves the lower bound value. We first factorize $W_j^* = \sum_{k=1}^d \tilde{u}_{jk} \tilde{v}_{jk}^T$. According to Theorem 3.3 in ((Mishkin et al., 2022)), for any $\{j, k\}$, under Assumption A.8, we can write $\tilde{u}_{jk} = \tilde{u}'_{jk} - \tilde{u}''_{jk}$ such that $\tilde{u}'_{jk}, \tilde{u}''_{jk} \in \mathcal{K}_j$ with $\mathcal{K}_j = \{u \in \mathbb{R}^d : (2D_j - I)Xu \succeq 0\}$. Therefore, when $m \geq 2Pd$, we can set $\{u_j, v_j\}$ to enumerate through $\{\tilde{u}'_{jk}, \tilde{v}_{jk}\}$ and $\{\tilde{u}''_{jk}, -\tilde{v}_{jk}\}$ to achieve optimal value of (5). With absolute value activation, replace D_j to be $\text{diag}(\text{sign}(Xu_j))$ with D_1, \dots, D_P enumerates all possible sign patterns of $\text{diag}(\text{sign}(Xu))$. \square

B. Supplementary Theoretic Materials for Section 4

B.1. Proof of Theorem 4.1

Consider data matrix $x \in \mathbb{R}^n$. Let m denote number of hidden neurons, then we have first layer weight $w \in \mathbb{R}^m$, first layer bias $b \in \mathbb{R}^m$, second layer weight $\alpha \in \mathbb{R}^m$ and second layer bias $b_0 \in \mathbb{R}$. Let l denotes the label vector, i.e. $l = [\delta_1/\epsilon, \delta_2/\epsilon, \dots, \delta_n/\epsilon]^T$. The score matching objective is reduced to

$$p^* = \min_{w, \alpha, b} \frac{1}{2} \left\| \sum_{j=1}^m (xw_j + 1b_j)_+ \alpha_j + 1b_0 - l \right\|_2^2 + \frac{1}{2} \beta \sum_{j=1}^m (w_j^2 + \alpha_j^2).$$

According to Lemma 2 in (Pilanci & Ergen, 2020), after rescaling, the above problem is equivalent to

$$\min_{\substack{w, \alpha, b \\ |w_j|=1}} \frac{1}{2} \left\| \sum_{j=1}^m (xw_j + 1b_j)_+ \alpha_j + 1b_0 - l \right\|_2^2 + \beta \sum_{j=1}^m |\alpha_j|,$$

which can be rewritten as

$$\begin{aligned} \min_{\substack{w, \alpha, b, r \\ |w_j|=1}} \frac{1}{2} \|r\|_2^2 + \beta \sum_{j=1}^m |\alpha_j| \\ \text{s.t. } r = \sum_{j=1}^m (xw_j + 1b_j)_+ \alpha_j + 1b_0 - l. \end{aligned} \quad (31)$$

The dual of problem (31) writes

$$\begin{aligned} d^* = \max_z -\frac{1}{2} \|z\|_2^2 + z^T l \\ \text{s.t. } \begin{cases} |z^T(x - 1x_i)_+| \leq \beta \\ |z^T(-x + 1x_i)_+| \leq \beta \\ z^T \mathbf{1} = 0 \end{cases} \quad \forall i = 1, \dots, n. \end{aligned}$$

Note the constraint set is strictly feasible since $z = 0$ always satisfies the constraints, Slater's condition holds and we get the dual problem as

$$d^* = \min_{\substack{z_0, z_1, z_2, z_3, z_4 \\ \text{s.t. } z_0, z_1, z_2, z_3 \geq 0}} \frac{1}{2} \|e\|_2^2 + f,$$

where $e = \sum_{i=1}^n z_{0i}(x - 1x_i)_+ - \sum_{i=1}^n z_{1i}(x - 1x_i)_+ + \sum_{i=1}^n z_{2i}(-x + 1x_i)_+ - \sum_{i=1}^n z_{3i}(-x + 1x_i)_+ + 1z_4 + l$ and $f = \beta(\|z_0\|_1 + \|z_1\|_1 + \|z_2\|_1 + \|z_3\|_1)$. Simplify to get

$$\min_y \frac{1}{2} \|Ay + \bar{l}\|_2^2 + \beta \|y\|_1,$$

with $A = [\bar{A}_1, \bar{A}_2] \in \mathbb{R}^{n \times 2n}$ where $\bar{A}_1 = (I - \frac{1}{n}11^T)A_1$, $\bar{A}_2 = (I - \frac{1}{n}11^T)A_2$ with $[A_1]_{ij} = (x_i - x_j)_+$ and $[A_2]_{ij} = (-x_i + x_j)_+$. $\bar{l}_j = l_j - \sum_i l_i/n$ is the mean-subtracted label vector. Once we obtain optimal solution y^* to problem (10), we can take

$$\begin{cases} w_j^* = \sqrt{|y_j^*|}, \alpha_j^* = -\sqrt{|y_j^*|}, b_j^* = -\sqrt{|y_j^*|}x_j \text{ for } j = 1, \dots, n, \\ w_j^* = -\sqrt{|y_j^*|}, \alpha_j^* = -\sqrt{|y_j^*|}, b_j^* = \sqrt{|y_j^*|}x_{j-n} \text{ for } j = n+1, \dots, 2n, \\ b_0^* = \frac{1}{n}1^T([A_1, A_2]y^* + l), \end{cases}$$

then denoising score matching objective has the same value as optimal value of convex program (10), which indicates $p^* = d^*$ and the above parameter set is optimal.

B.2. Convex Programs for Univariate Data with More Model Architectures

B.2.1. ABSOLUTE VALUE ACTIVATION WITHOUT SKIP CONNECTION

Theorem B.1. When σ is absolute value activation and $V = 0$, denote the optimal score matching objective value (9) with s_θ specified in (3) as p^* , when $\beta > 0$ and $m \geq m^*$,

$$p^* = \min_y \frac{1}{2} \|Ay + b\|_2^2 + \beta \|y\|_1, \quad (32)$$

where $m^* = \|y^*\|_0$, and y^* is any optimal solution to (32). A, b and reconstruction rule for θ is specified in the proof below.

Proof. Consider data matrix $x \in \mathbb{R}^n$. Let m denote number of hidden neurons, then we have first layer weight $w \in \mathbb{R}^m$, first layer bias $b \in \mathbb{R}^m$, second layer weight $\alpha \in \mathbb{R}^m$ and second layer bias $b_0 \in \mathbb{R}$. Let l denotes the label vector, i.e. $l = [\delta_1/\epsilon, \delta_2/\epsilon, \dots, \delta_n/\epsilon]^T$. The score matching objective is reduced to

$$p^* = \min_{w, \alpha, b} \frac{1}{2} \left\| \sum_{j=1}^m (xw_j + 1b_j)_+ \alpha_j + 1b_0 - l \right\|_2^2 + \frac{1}{2} \beta \sum_{j=1}^m (w_j^2 + \alpha_j^2).$$

According to Lemma 2 in (Pilanci & Ergen, 2020), after rescaling, the above problem is equivalent to

$$\min_{\substack{w, \alpha, b \\ |w_j|=1}} \frac{1}{2} \left\| \sum_{j=1}^m (xw_j + 1b_j)_+ \alpha_j + 1b_0 - l \right\|_2^2 + \beta \sum_{j=1}^m |\alpha_j|,$$

which can be rewritten as

$$\begin{aligned} & \min_{\substack{w, \alpha, b, r \\ |w_j|=1}} \frac{1}{2} \|r\|_2^2 + \beta \sum_{j=1}^m |\alpha_j| \\ & \text{s.t. } r = \sum_{j=1}^m (xw_j + 1b_j)_+ \alpha_j + 1b_0 - l. \end{aligned} \quad (33)$$

The dual of problem (33) writes

$$\begin{aligned} d^* &= \max_z -\frac{1}{2} \|z\|_2^2 + z^T l \\ & \text{s.t. } \begin{cases} |z^T(x - 1x_i)_+| \leq \beta \\ |z^T(-x + 1x_i)_+| \leq \beta \\ z^T 1 = 0 \end{cases} \quad \forall i = 1, \dots, n. \end{aligned}$$

Note the constraint set is strictly feasible since $z = 0$ always satisfies the constraints, Slater's condition holds and we get the dual problem as

$$d^* = \min_{z_0, z_1, z_2, z_3, z_4} \frac{1}{2} \|e\|_2^2 + f, \\ \text{s.t. } z_0, z_1, z_2, z_3 \geq 0$$

where $e = \sum_{i=1}^n z_{0i}(x - 1x_i)_+ - \sum_{i=1}^n z_{1i}(x - 1x_i)_+ + \sum_{i=1}^n z_{2i}(-x + 1x_i)_+ - \sum_{i=1}^n z_{3i}(-x + 1x_i)_+ + 1z_4 + l$ and $f = \beta(\|z_0\|_1 + \|z_1\|_1 + \|z_2\|_1 + \|z_3\|_1)$. Simplify to get

$$\min_y \frac{1}{2} \|Ay + \bar{l}\|_2^2 + \beta \|y\|_1.$$

where $A = (I - \frac{1}{n}11^T) A_3 \in \mathbb{R}^{n \times n}$ with $[A_3]_{ij} = |x_i - x_j|$, \bar{l} is the same as defined in Appendix B.1. Once we obtain optimal solution y^* to problem (32), we can take

$$\begin{cases} w_j^* = \sqrt{|y_j^*|}, \alpha_j^* = -\sqrt{|y_j^*|}, b_j^* = -\sqrt{|y_j^*|}x_j \text{ for } j = 1, \dots, n, \\ w_j^* = -\sqrt{|y_j^*|}, \alpha_j^* = -\sqrt{|y_j^*|}, b_j^* = \sqrt{|y_j^*|}x_{j-n} \text{ for } j = n+1, \dots, 2n, \\ b_0^* = \frac{1}{n}1^T([A_1, A_2]y^* + l), \end{cases}$$

then denoising score matching objective has the same value as optimal value of convex program (32), which indicates $p^* = d^*$ and the above parameter set is optimal. \square

B.2.2. RELU ACTIVATION WITH SKIP CONNECTION

Theorem B.2. When σ is ReLU and $V \neq 0$, denote the optimal score matching objective value (9) with s_θ specified in (3) as p^* , when $\beta > 0$ and $m \geq m^*$,

$$p^* = \min_y \frac{1}{2} \|Ay + b\|_2^2 + 2\beta \|y\|_1, \quad (34)$$

where $m^* = \|y^*\|_0$, and y^* is any optimal solution to (34). A, b and reconstruction rule for θ is specified in the proof below.

Proof. Following proof logic in Appendix A.3.3, let $\{w^r, b^r, \alpha^r, v^r\}$ denotes parameter set corresponding to ReLU activation with skip connection, consider another parameter set $\{w^a, b^a, \alpha^a, z^a\}$ satisfying

$$\begin{cases} \alpha^r = 2\alpha^a, \\ w^r = w^a, \\ b^r = b^a, \\ b_0^r = b_0^a - \frac{1}{2} \sum_{j=1}^m b_j^r \alpha_j^r, \\ v^r = v^a - \frac{1}{2} \sum_{j=1}^m W_j^r \alpha_j^r. \end{cases}$$

Then the denoising score matching objective

$$\min_{w^r, \alpha^r, b^r, v^r} \frac{1}{2} \left\| \sum_{j=1}^m (xw_j^r + 1b_j^r)_+ \alpha_j^r + xv^r + 1b_0^r - l \right\|_2^2 + \frac{\beta}{2} \sum_{j=1}^m (w_j^{r2} + \alpha_j^{r2})$$

is equivalent to

$$\min_{w^a, \alpha^a, b^a, v^a} \frac{1}{2} \left\| \sum_{j=1}^m |xw_j^a + 1b_j^a| \alpha_j^a + xv^a + 1b_0^a - l \right\|_2^2 + \frac{\beta}{2} \sum_{j=1}^m (w_j^{a2} + 4\alpha_j^{a2}).$$

According to Lemma 2 in (Pilanci & Ergen, 2020), after rescaling, the above problem is equivalent to

$$\min_{\substack{w^a, \alpha^a, b^a, v^a \\ |w_j^a|=1}} \frac{1}{2} \left\| \sum_{j=1}^m |xw_j^a + 1b_j^a| \alpha_j^a + xv^a + 1b_0^a - l \right\|_2^2 + 2\beta \sum_{j=1}^m |\alpha_j^a|. \quad (35)$$

Following similar analysis as in Appendix B.2.3 with a different rescaling factor, the optimal solution set to (35) is given by

$$\begin{cases} w_j^{a*} = \sqrt{2|y_j^*|}, \alpha_j^{a*} = -\sqrt{|y_j^*|/2}, b_j^{a*} = -\sqrt{2|y_j^*|}x_j \text{ for } j = 1, \dots, n, \\ w_j^{a*} = -\sqrt{2|y_j^*|}, \alpha_j^{a*} = -\sqrt{|y_j^*|/2}, b_j^{a*} = \sqrt{2|y_j^*|}x_{j-n} \text{ for } j = n+1, \dots, 2n, \\ v^{a*} = \bar{x}^T((I - \frac{1}{n}11^T)A_3y^* + \bar{l})/\|\bar{x}\|_2^2, \\ b_0^{a*} = \frac{1}{n}1^T(A_3y^* - xv^{a*} + l), \end{cases}$$

where y^* is optimal solution to convex program (34). Then the optimal parameter set $\{w^r, b^r, \alpha^r, v^r\}$ is given by

$$\begin{cases} w_j^{r*} = \sqrt{2|y_j^*|}, \alpha_j^{r*} = -\sqrt{2|y_j^*|}, b_j^{r*} = -\sqrt{2|y_j^*|}x_j \text{ for } j = 1, \dots, n, \\ w_j^{r*} = -\sqrt{2|y_j^*|}, \alpha_j^{r*} = -\sqrt{2|y_j^*|}, b_j^{r*} = \sqrt{2|y_j^*|}x_{j-n} \text{ for } j = n+1, \dots, 2n, \\ v^{r*} = \bar{x}^T((I - \frac{1}{n}11^T)A_3y^* + \bar{l})/\|\bar{x}\|_2^2 - \sum_{j=1}^m w_j^{r*}\alpha_j^{r*}/2, \\ b_0^{r*} = \frac{1}{n}1^T(A_3y^* - x(\bar{x}^T((I - \frac{1}{n}11^T)A_3y^* + \bar{l})/\|\bar{x}\|_2^2) + l) - \sum_{j=1}^m b_j^{r*}\alpha_j^{r*}/2. \end{cases}$$

Note in convex program (34), $A = B^{\frac{1}{2}}(I - \frac{1}{n}11^T)A_3 \in \mathbb{R}^{n \times n}$, $b = B^{\frac{1}{2}}\bar{l} \in \mathbb{R}^n$ where $B = I - P_{\bar{x}}$ with $P_{\bar{x}} = \bar{x}\bar{x}^T/\|\bar{x}\|_2^2$ and \bar{x} being the mean-subtracted data vector as defined in Section A.3.3. A_3 and \bar{l} are the same as defined in Appendix B.2.1. \square

B.2.3. ABSOLUTE VALUE ACTIVATION WITH SKIP CONNECTION

Theorem B.3. When σ is absolute value activation and $V \neq 0$, denote the optimal score matching objective value (9) with s_θ specified in (3) as p^* , when $\beta > 0$ and $m \geq m^*$,

$$p^* = \min_y \frac{1}{2}\|Ay + b\|_2^2 + \beta\|y\|_1, \quad (36)$$

where $m^* = \|y^*\|_0$, and y^* is any optimal solution to (36). A, b and reconstruction rule for θ is specified in the proof below.

Proof. Consider data matrix $x \in \mathbb{R}^n$. Let m denote number of hidden neurons, then we have first layer weight $w \in \mathbb{R}^m$, first layer bias $b \in \mathbb{R}^m$, second layer weight $\alpha \in \mathbb{R}^m$, second layer bias $b_0 \in \mathbb{R}$, and skip connection v . Let l denotes the label vector, i.e, $l = [\delta_1/\epsilon, \delta_2/\epsilon, \dots, \delta_n/\epsilon]^T$. The score matching objective is reduced to

$$p^* = \min_{w, \alpha, b, v} \frac{1}{2} \left\| \sum_{j=1}^m |xw_j + 1b_j|\alpha_j + xv + 1b_0 - l \right\|_2^2 + \frac{1}{2}\beta \sum_{j=1}^m (w_j^2 + \alpha_j^2).$$

After applying the rescaling strategy as in (Pilanci & Ergen, 2020), the above problem is equivalent to

$$\begin{aligned} \min_{\substack{w, \alpha, b, v, r \\ |w_j|=1}} \frac{1}{2}\|r\|_2^2 + \beta \sum_{j=1}^m |\alpha_j| \\ \text{s.t. } r = \sum_{j=1}^m |xw_j + 1b_j|\alpha_j + xv + 1b_0 - l. \end{aligned}$$

The dual problem is given by

$$\begin{aligned} d^* = \max_z -\frac{1}{2}\|z\|_2^2 + z^T l \\ \text{s.t. } \begin{cases} |z^T|x - 1x_i| \leq \beta \\ |z^T| - x + 1x_i| \leq \beta \\ z^T \mathbf{1} = 0 \\ z^T x = 0 \end{cases} \quad \forall i = 1, \dots, n, \end{aligned}$$

which gives a lower bound of p^* . Note the constraint set is satisfied by taking $z = 0$, thus Slater's condition holds and the dual problem is given by

$$d^* = \min_{y_1, y_2, y_3} \frac{1}{2} \|A_3 y_1 + x y_2 + 1 y_3 + l\|_2^2 + \beta \|y_1\|_1.$$

Minimizing over y_2 and y_3 gives the optimal $y_3^* = -1^T(A_3 y_1 + x y_2 + l)/n$ and $y_2^* = -\bar{x}^T((I - \frac{1}{n}11^T)A_3 y_1 + \bar{l})/\|\bar{x}\|_2^2$ and the above problem is equivalent to

$$\min_{y_1} \frac{1}{2} \|A y_1 + b\|_2^2 + \beta \|y_1\|_1,$$

where A, b are the same as defined in Appendix B.2.2. Once we obtain optimal solution y^* to problem (36), we can take

$$\begin{cases} w_j^* = \sqrt{|y_j^*|}, \alpha_j^* = -\sqrt{|y_j^*|}, b_j^* = -\sqrt{|y_j^*|} x_j \text{ for } j = 1, \dots, n, \\ v^* = \bar{x}^T((I - \frac{1}{n}11^T)A_3 y^* + \bar{l})/\|\bar{x}\|_2^2, \\ b_0^* = \frac{1}{n}1^T(A_3 y^* - x v^* + l), \end{cases}$$

then denoising score matching objective has the same value as optimal value of convex program (36), which indicates $p^* = d^*$ and the above parameter set is optimal. \square

B.3. Proof of Theorem 4.2

Proof. When $X \in \mathbb{R}^{n \times d}$ for some $d > 1$, when $\beta = 0$, the score matching objective can be reduced to

$$p^* = \min_{u_j, v_j} \sum_{i=1}^n \frac{1}{2} \left\| \sum_{j=1}^m (X_i u_j)_+ v_j^T - L_i \right\|_2^2,$$

which can be rewritten as

$$\min_{u_j, v_j} \frac{1}{2} \left\| \sum_{j=1}^m (X u_j)_+ v_j^T - Y \right\|_F^2. \quad (37)$$

Let $D'_j = \text{diag}(\mathbb{1}\{X u_j \geq 0\})$, then problem (37) is equivalent to

$$\min_{u_j, v_j} \frac{1}{2} \left\| \sum_{j=1}^m D'_j X u_j v_j^T - Y \right\|_F^2.$$

Therefore,

$$\begin{aligned} p^* &= \min_{\substack{W_j = u_j v_j^T \\ (2D'_j - I)X u_j \geq 0}} \frac{1}{2} \left\| \sum_{j=1}^m D'_j X W_j - Y \right\|_F^2 \\ &\geq \min_{W_j} \frac{1}{2} \left\| \sum_{j=1}^P D_j X W_j - Y \right\|_F^2, \end{aligned}$$

where D_1, \dots, D_P enumerates all possible sign patterns of $\text{diag}(\mathbb{1}\{X u \geq 0\})$. Under Assumption A.8, the construction of optimal parameter set follows Appendix A.9.1. With absolute value activation, replace D'_j to be $\text{diag}(\text{sign}(X u_j))$ and the constraints in 29 become $W_j = u_j v_j^T, D'_j X u_j \geq 0$, and D_1, \dots, D_P enumerates all possible sign patterns of $\text{diag}(\text{sign}(X u))$. \square

C. Supplementary Simulation Results

In this section, we give more simulation results besides those discussed in main text in Section 5. In Section C.1 we show simulation results for score matching tasks with more neural network types and data distributions. In section C.2 we show simulation results for denoising score matching tasks with more neural network types.

C.1. Score Matching Simulations

Figure 7 shows our experimental results with data uniformly distributed on $[0, 1]$. Note our convex score predictor produces the optimal training loss and the predicted score is aligned with our analysis in Section 3.3. Figure 8, 9, and 10 below show

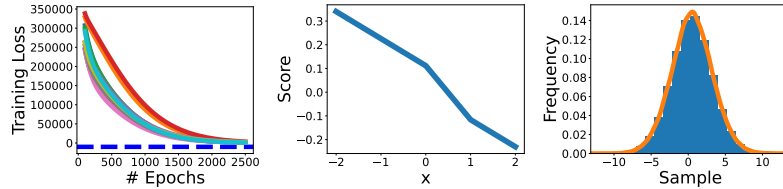


Figure 7. Simulation results for score matching tasks with two-layer ReLU neural network (Uniform data). The left plot shows training loss where the dashed blue line indicates loss of convex score predictor (4). The middle plot shows score prediction by convex score predictor, which confirms our analysis in Section 3.3. The right plot shows sampling histogram via Langevin process with convex score predictor. Here the predicted score function is still close to score of Gaussian, which is due to the large weight decay, see Section 3.3 for details.

simulation results for score matching tasks with neural network of different types. In Figure 8, we show simulation results for neural network with absolute value activation and without skip connection. We use the same data samples and training parameters as explained in Section 5.1. The gap between non-convex training loss and convex score predictor loss can be due to the non-smoothness threshold function in the score matching training objective. The score prediction in the middle plot is aligned with our theoretic result in Section 3.3 and the sampling histogram in the right plot is consistent with the score prediction. In Figure 9 and 10, we set the weight decay parameter to $\beta = \|b\|_\infty + 1$.⁶ Data samples and the rest training parameters are the same as in Section 5.1. Figure 9 shows results for two-layer ReLU network with skip connection and Figure 10 shows results for neural network with absolute value activation and with skip connection. Interestingly, the gap between non-convex training loss and convex score predictor loss is minor compared to Figure 8. The predicted score functions are linear with slope close to minus one over sample variance and interception close to sample mean, i.e., -1 and 0 respectively. This is aligned with our theoretic result in Appendix A.6.2 and A.6.3. The sampling histograms are consistent with the score prediction.

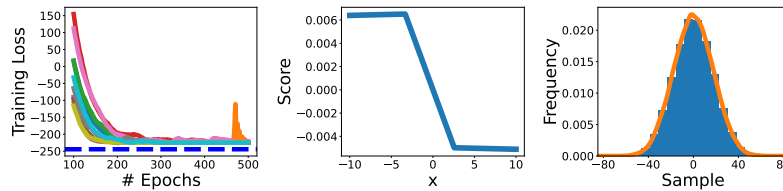


Figure 8. Simulation results for score matching tasks with two-layer neural network with absolute value activation and no skip connection. The left plot shows training loss where the dashed blue line indicates loss of convex score predictor (14). The middle plot shows score prediction from convex score predictor, which confirms our analysis in Section 3.3. The right plot shows sampling histogram via Langevin process with convex score predictor. The ground truth distribution is standard Gaussian.

C.2. Denoising Score Matching Simulations

In annealed Langevin sampling procedure, s_{θ_i} for $i = 1, 2, \dots, L$ are neural networks trained for denoising score matching with different noise scales. Specifically, we take $L = 10, T = 10, \epsilon_0 = 2e - 5, [\sigma_1, \dots, \sigma_L]$ being the uniform grid from 1 to 0.01, and μ_0 being uniform distribution from -1 to 1. Figure 11, 12, and 13 below show simulation results for denoising score matching tasks for neural network of different types. We use the same simulation parameters as described in Section 5. The upper left plots in these three figures show the training loss where the dashed blue line is the objective value obtained by convex score predictors. The gap between non-convex training loss and convex score predictor loss indicates that our convex program solves the training problem globally. The first histograms in these three figures show sampling histograms via annealed Langevin process with convex score estimator. Since the ground truth distribution is standard Gaussian, our convex

⁶See Section A.3 for definition of b .

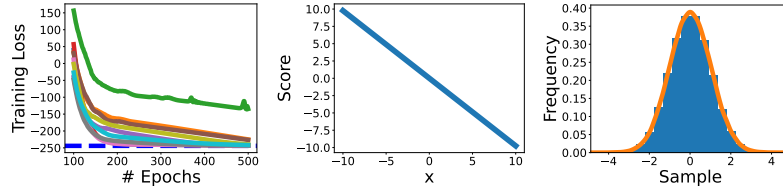


Figure 9. Simulation results for score matching tasks with two-layer ReLU neural network with skip connection. The left plot shows training loss where the dashed blue line indicates loss of convex score predictor (18). The middle plot shows score prediction from convex score predictor, which confirms our analysis in Appendix A.6.2. The right plot shows sampling histogram via Langevin process with convex score predictor. The ground truth distribution is standard Gaussian.

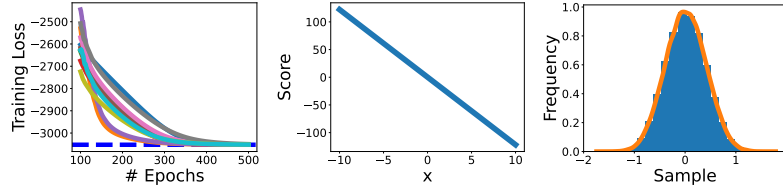


Figure 10. Simulation results for score matching tasks with two-layer neural network with absolute value activation and skip connection. The left plot shows training loss where the dashed blue line indicates loss of convex score predictor (20). The middle plot shows score prediction from convex score predictor, which confirms our analysis in Appendix A.6.3. The right plot shows sampling histogram via Langevin process with convex score predictor. The ground truth distribution is standard Gaussian.

programs recover the ground truth data distribution. The rest histograms in these three figures are sampling results with non-convex score predictors corresponding to different learning rates, as what can be observed, the result relies heavily on learning rate choices and thus may not be stable.

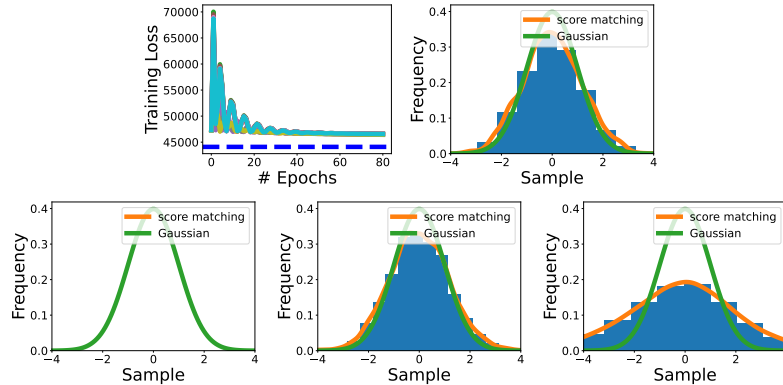


Figure 11. Simulation results for denoising score matching tasks with neural network with absolute value activation and no skip connection. The upper left plot shows training loss where the dashed blue line indicates loss of convex score predictor (32). The second plot shows sampling histogram via annealed Langevin process with convex score predictor. The third, fourth, fifth plots show sampling histograms via annealed Langevin process with non-convex score predictors trained with learning rates $1, 1e - 2, 1e - 6$ respectively. The ground truth distribution is standard Gaussian, which is recovered by our model.

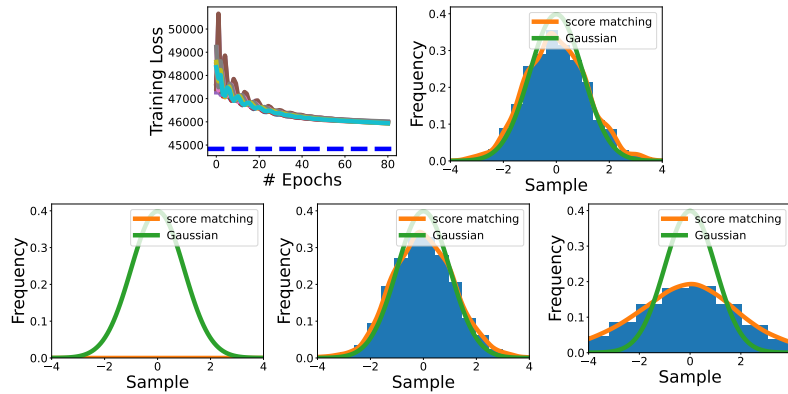


Figure 12. Simulation results for denoising score matching tasks with neural network with ReLU activation and skip connection. The upper left plot shows training loss where the dashed blue line indicates loss of convex score predictor (34). The second plot shows sampling histogram via annealed Langevin process with convex score predictor. The third, fourth, fifth plots show sampling histograms via annealed Langevin process with non-convex score predictors trained with learning rates $1, 1e - 2, 1e - 6$ respectively. The ground truth distribution is standard Gaussian, which is recovered by our model.

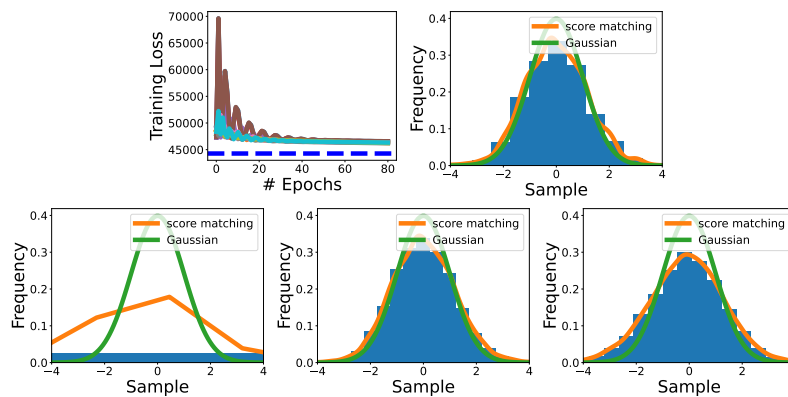


Figure 13. Simulation results for denoising score matching tasks with neural network with absolute value activation and skip connection. The upper left plot shows training loss where the dashed blue line indicates loss of convex score predictor (36). The second plot shows sampling histogram via annealed Langevin process with convex score predictor. The third, fourth, fifth plots show sampling histograms via annealed Langevin process with non-convex score predictors trained with learning rates $1, 1e - 2, 1e - 6$ respectively. The ground truth distribution is standard Gaussian, which is recovered by our model.